Measuring vertical tectonic motion at the intersection of the Santa Cruz–Catalina Ridge and Northern Channel Islands platform, California Continental Borderland, using submerged paleoshorelines

Jason D. Chaytor[†§]
Chris Goldfinger
Melissa A. Meiner[#]
College of Oceanic and Atmospheric Sciences, Oregon State University, 104 Ocean Administration Building, Corvallis, Oregon 97331, USA

Gary J. Huftile
School of Natural Resource Sciences, Queensland University of Technology, 2 George Street, Brisbane, QLD 4001, Australia

Christopher G. Romsos
College of Oceanic and Atmospheric Sciences, Oregon State University, 104 Ocean Administration Building, Corvallis, Oregon 97331, USA

Mark R. Legg
Legg Geophysical, Huntington Beach, California 92647, USA

ABSTRACT

We used submerged paleoshorelines as strain markers to investigate Holocene and late Pleistocene vertical tectonic movement at the intersection of the offshore Santa Cruz–Catalina Ridge with the southern boundary of the Western Transverse Ranges, within the California Continental Borderland. Past submerged shoreline positions were identified using high-resolution multibeam bathymetry, side-scan sonar, submersible observations, and the presence of intertidal and subtidal invertebrate fossils. Numerous accelerator mass spectrometry (AMS) ^{14}C ages of shells from these paleoshorelines were found to be between ~27,000 yr radiocarbon (RC) and 11,500 yr before present, indicative of shoreline colonization during and following the Last Glacial Maximum (LGM), establishing these paleoshorelines as a usable datum for measuring vertical change since this time. Removal of the nontectonic component of vertical change using an ice-volume-equivalent eustatic sea-level compilation indicates between 20 and 45 m of uplift of the eastern part of the Northern Channel Islands block since the LGM lowstand, resulting in an uplift rate of 1.50 ± 0.59 mm/yr over the last 23 k.y. This rate closely matches uplift predicted by published slip rates for the Channel Islands thrust, which underlies the Northern Channel Islands platform. Results from post-LGM shoreline features on Pilgrim Banks are somewhat more ambiguous. Submarine paleoshoreline uplift, together with the extensive upper-crustal fold-thrust style of deformation, illustrates the transpressional interaction of the Borderland and the Western Transverse Ranges blocks where the Santa Cruz–Catalina Ridge and northern Channel Islands intersect.

Keywords: Bathymetry, submersibles, radiocarbon dating, structural geology, sea level.

INTRODUCTION

Uplifted and submerged terraces have proved to be valuable recorders of vertical tectonic motion in many locations around the world (e.g., Lajoie, 1986; Dickinson, 2001; Webster et al., 2004), and notably in several locations around coastal southern California (Orr, 1960; Muhs, 1983; Ward and Valensise, 1994; Pinter et al., 1998). On the mainland shelf and offshore islands and banks throughout the California Borderland (Fig. 1A), evidence of the Last Glacial Maximum (LGM) sea-level lowstand shelf planation is strikingly evident, with the depth of these prominent shelf breaks varying between 30 to >140 m. The variation in depth of these potentially correlatable shelf breaks from the depth expected from eustatic sea-level change alone can reveal the magnitude and spatial variability of the Holocene–late Pleistocene vertical motion within this tectonically active region.

The amount and rate of vertical motion recorded by the paleoshorelines in southern California have the potential to provide information on fault kinematics and, more importantly, constraints on slip rates on faults at structural intersections that are critical for earthquake hazard analysis. In southern California and other highly populated regions, large earthquakes at the intersection of active structural domains pose a significant hazard. An understanding of the deformation history and the future earthquake potential of the individual faults within the intersecting structural systems is critical in determining the seismic hazards that these regions pose. Two key components in illuminating these hazards are (1) determining the amount of accumulated displacement and recency of movement along each of the intersecting fault systems, and (2) understanding how the displacement is accommodated, be it through transfer of motion to numerous smaller surrounding structures,

[†]E-mail: jchaytor@whoi.edu
[§]Present address: Department of Geology and Geophysics, Woods Hole Oceanographic Institution, MS 24, Woods Hole, Massachusetts 02543, USA.
[#]Present address: Department of Geology, University of Hawaii at Hilo, 200 W. Kawili Street, Hilo, Hawaii 96720, USA.

GSA Bulletin; July/August 2008; v. 120; no. 7/8; p. 1053–1071; doi: 10.1130/B26316.1; 10 figures; 1 table.

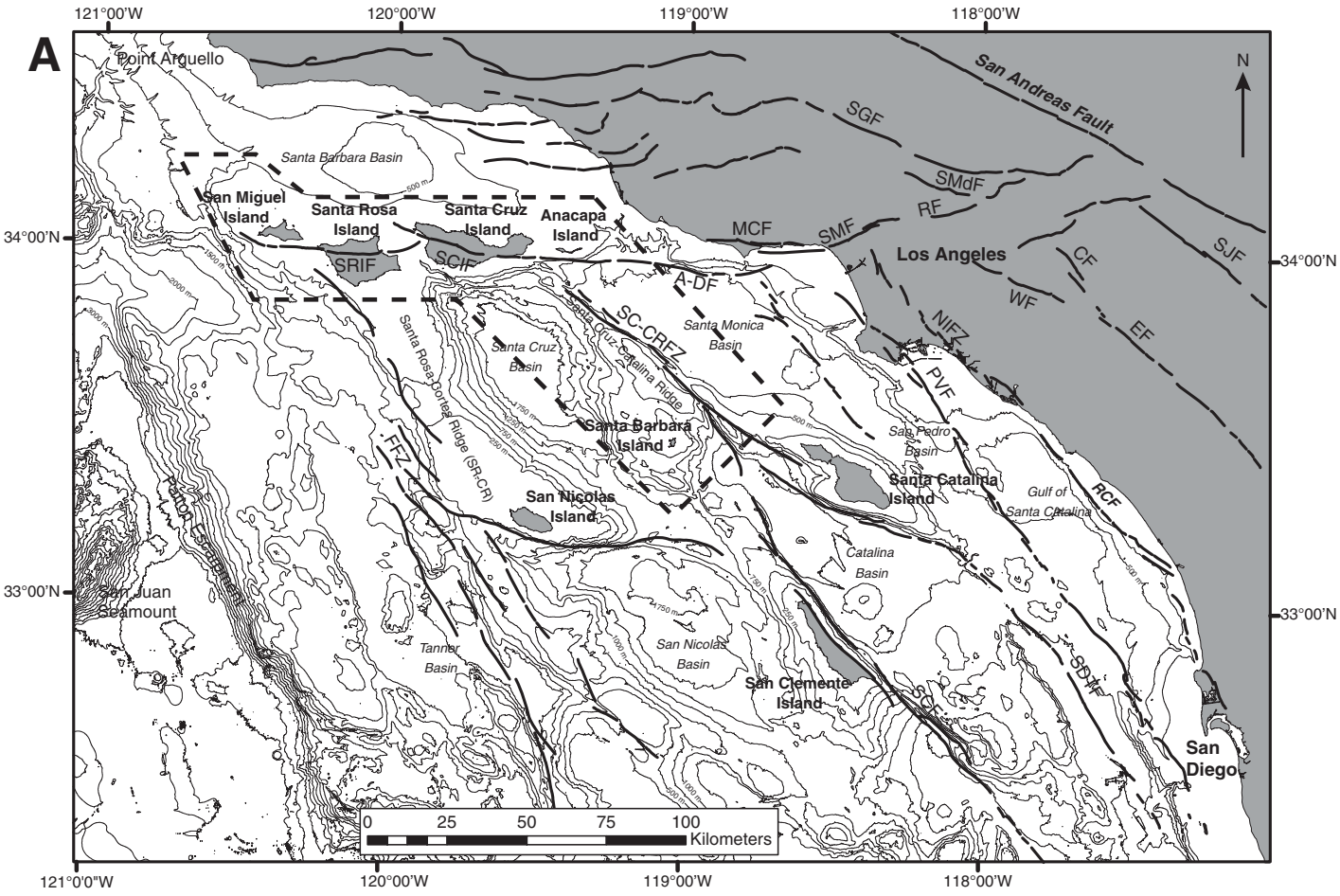

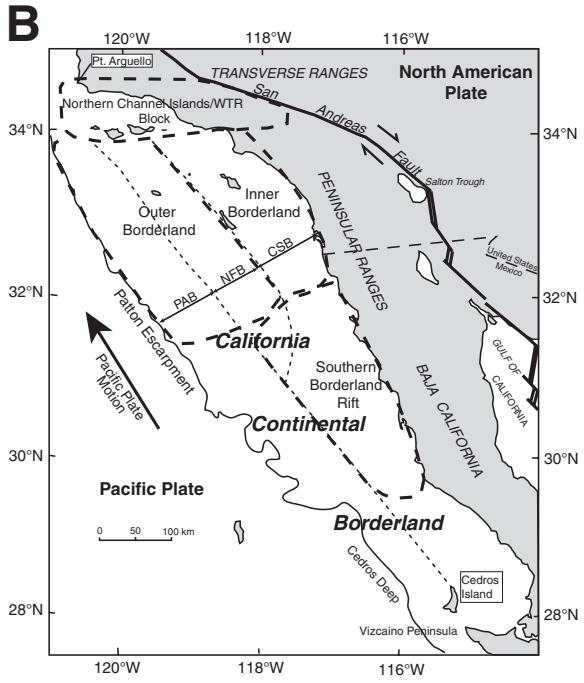

Figure 1. (A) Map of the California Continental Borderland, offshore southern California, based on compiled multibeam data. The primary focus area of this study, the Santa Cruz–Catalina Ridge and the Northern Channel Islands platform, are enclosed by the dashed polygon. The depth contour interval is 250 m. Traces of onshore and offshore faults from Jennings (1994) are shown with the major faults and fault zones labeled: A-DF—Anacapa-Dume fault; CF—Chino fault; EF—Elsinore fault; FFZ—Ferrelo fault zone; MCF—Malibu Coast fault; NIFZ—Newport-Inglewood fault zone; PVF—Palos Verdes fault; RCF—Rose Canyon fault; RF—Raymond fault; SC-CRFZ—Santa Cruz–Catalina Ridge fault zone; SCF—San Cayetano fault; SCIF—Santa Cruz Island fault; SGF—San Gabriel fault; SJF—San Jacinto fault; SMF—Santa Monica fault; SMdF—Sierra Madre fault; SRIF—Santa Rosa Island fault; WF—Whittier fault. (B) Tectonic setting of the California Continental Borderland, which extends from Point Arguello to Cedros Island. The various post-Oligocene tectonic terranes that constitute the southern California Borderland—i.e., the Inner and Outer Borderland, Southern Borderland Rift, and Northern Channel Islands–Western Transverse Ranges (WTR) blocks—are indicated by thick dashed lines. Thinner dashed lines and arrows indicate lithostratigraphic terranes of Vedder (1987). PAB—Patton Accretionary Complex; NFB—Nicolas Forearc Belt; CSB—Catalina Schist Belt. Modified from Legg (1991a).

broader-scale horizontal and vertical tectonic accommodation, continuation of individual structures beyond the intersecting boundaries, or some combination of these mechanisms.

One of the most urbanized regions of actively intersecting structural and tectonic blocks occurs where the east-west–trending transpressional structures of the Transverse Ranges Province intersect the northwest-southeast–striking faults of the Peninsular Ranges and Borderland at an angle of ~45° (Fig. 1A). Using the known structural architecture of the region, several hypotheses have been proposed to explain how the major northwest-striking right-lateral and right-oblique faults west of the San Andreas fault, such as the Santa Cruz–Catalina Ridge, Palos Verdes, Newport-Inglewood, and Elsinore fault systems, interact with major range-front thrust and left-lateral faults (Santa Monica, Anacapa-Dume, and Channel Islands faults) along the southern boundary of the Transverse Ranges. The dominant hypotheses include (1) complete underthrusting of the Peninsular Ranges Province below the Transverse Ranges Province (e.g., Namson and Davis, 1988; Sorlien et al., 2001; Legg et al., 2004) with continuation of the major structures beyond the intersection (e.g., Goldfinger et al., 1997; Legg et al., 2004); (2) termination of the major structures, and displacement transfer to numerous small faults and folds in the intersection zone (e.g., Tsutsumi et al., 2001; Legg et al., 2004); or (3) a combination of both.

Whereas previous investigations of this intersection zone have been focused on the onshore portion of the province boundaries, predominantly in the northern Los Angeles basin, for which extensive petroleum exploration data are available (e.g., Wright, 1991; Tsutsumi et al., 2001), many of the major structural components are poorly expressed at the surface, or in part are hidden by the extreme urbanization of the Los Angeles region. Because of this, we focus our investigation on the structural features along the section of this boundary within the California Continental Borderland, offshore of southern California, where the intersections are relatively well expressed and accessible using marine geophysical imaging and submarine observation and sampling. In this paper we test the above hypotheses of structural interaction, using elevation changes of lowstand submarine paleoshoreline features dated by ages derived from intertidal shells as a proxy for vertical tectonic uplift and fault slip rate where the Santa Cruz–Catalina Ridge intersects the Transverse Ranges Province at the Northern Channel Islands platform (composed of the Santa Cruz, Santa Rosa, San Miguel, and Anacapa Islands and their surrounding submerged shelf; Fig. 1A).

Physiography

The California Continental Borderland, as defined by Shepard and Emery (1941) and Moore (1969), is a predominantly submarine ridge-basin physiographic province that extends from Point Arguello in the north to Cedros Island off Baja California (Figs. 1A and 1B). The western edge of the region, which is as much as 250 km from the coast, is marked by the Patton Escarpment in the north and the Cedros Deep in the south. The Borderland is commonly divided into three subregions (Fig. 1B) on the basis of dominant structural trends, gravity and seismic-reflection signatures, and distribution of pre-Neogene rocks (e.g., Crouch, 1979; Teng and Gorsline, 1991; ten Brink et al., 2000). These regions are (1) Western Transverse Ranges block, the northern zone of west-trending structures including the Santa Barbara basin, and Northern Channel Islands platform; (2) the Inner Borderland, defined as the region of northwest-trending ridges and basins between the coast and the faults west of San Clemente Island, floored by rocks characteristic of the Franciscan Complex (Catalina Schist Belt of Vedder, 1987); and (3) the Outer Borderland, also characterized by northwest-trending structural and geomorphic features, with Neogene sedimentary and volcanic units overlying the Nicolas Forearc (Great Valley Sequence) and Patton Accretionary belts (Crouch, 1979; Vedder, 1987).

Tectonic Setting

The Borderland is a complex tectonic region that resulted from rapid shifts from subduction to rifting, plate fragmentation and capture, large-scale block rotation, and transtension to transpression over the last 30 m.y. (Yeats, 1968; Atwater, 1970; Dickinson and Snyder, 1979; Crouch and Suppe, 1993; Nicholson et al., 1994). The current phase of tectonic deformation, initiated at ca. 5–8 Ma (Curray and Moore, 1984; Engebretson et al., 1985; Atwater and Stock, 1998), followed a major shift in Pacific plate motion from a northwest-oriented direction to a more northerly direction. This shift localized the accommodation of enhanced dextral shear strain onto discrete fault zones such as the Santa Cruz–Catalina fault zone, formed within the larger Peninsular Ranges and Borderland blocks (e.g., Yeats, 1973). A slowing of the rotation of the Transverse Ranges block in the Pliocene (ca. 3.5 Ma; Wright, 1991) led to the initiation of a transpressive deformation field dominated by north-south to northeast-southwest crustal shortening (Yeats, 1983; Hauksson, 1990; Tsutsumi et al., 2001) and the development of south-vergent thrusting and left-oblique faulting in the Transverse Ranges and continued motion on the right-slip and right-oblique faults of the Peninsular Ranges and California Borderland (Wright, 1991).

Physical Oceanography

Oceanographic conditions in the California Borderland are dominated by components of the California current system, specifically the southern California countercurrent, undercurrent, eddy (Lynn and Simpson, 1990; Bray et al., 1999). Except in spring, poleward flow of surface water dominates east of the Santa Rosa–Cortes Ridge (Fig. 1A) and tends to flow over ridges and around islands (Dailey et al., 1993), with equatorial flow dominating west of the ridge. Below the surface flow the California undercurrent has a net poleward flow that is weaker over shelf areas in comparison with basin and slope regions, where it can reach velocities as high as 10–20 cm/s over slopes (Hickey, 1992). The overall circulation pattern directs suspended sediment toward the northernmost basin (Santa Barbara basin), with sufficient velocity to winnow silt and fine sands off the shelf (Gorsline and Teng, 1989). Waves enter the Borderland from the south in summer and from the north during the remainder of the year, creating a dominant southward-oriented longshore drift along the coast and shadow zones behind the islands for most of the year (Gorsline and Teng, 1989; Dailey et al., 1993). Only periodically occurring large storm waves are able to mix bottom sediments on the shallow shelf. Terrigenous clastic sediments tend to be trapped along the mainland shelves so that islands, ridges, and banks are relatively free of the fine-grained terrigenous material. Wave action and tidal currents further winnow the fines on the shallow offshore areas, while hemipelagic mud drapes the deeper slopes and basin areas.

Structural Components of the Onshore and Offshore Intersections

In southern California, numerous major onshore and offshore right-lateral fault systems interact in a complex way with left-lateral strike-slip and north-dipping thrust faults along the boundary between the Transverse Ranges and Peninsular Ranges provinces (Fig. 2; Wright, 1991 and references within; Stephenson et al., 1995; Dolan et al., 2000a, 2000b; Tsutsumi et al., 2001; Yeats, 2004; Fisher et al., 2005a). Within the Borderland the major northwest-striking right-lateral faults are found within the San Pedro basin (Fisher et al., 2003; Legg et al., 2004) and along the Santa Cruz–Catalina Ridge and Ferrelo fault zones (Santa Rosa–Cortes

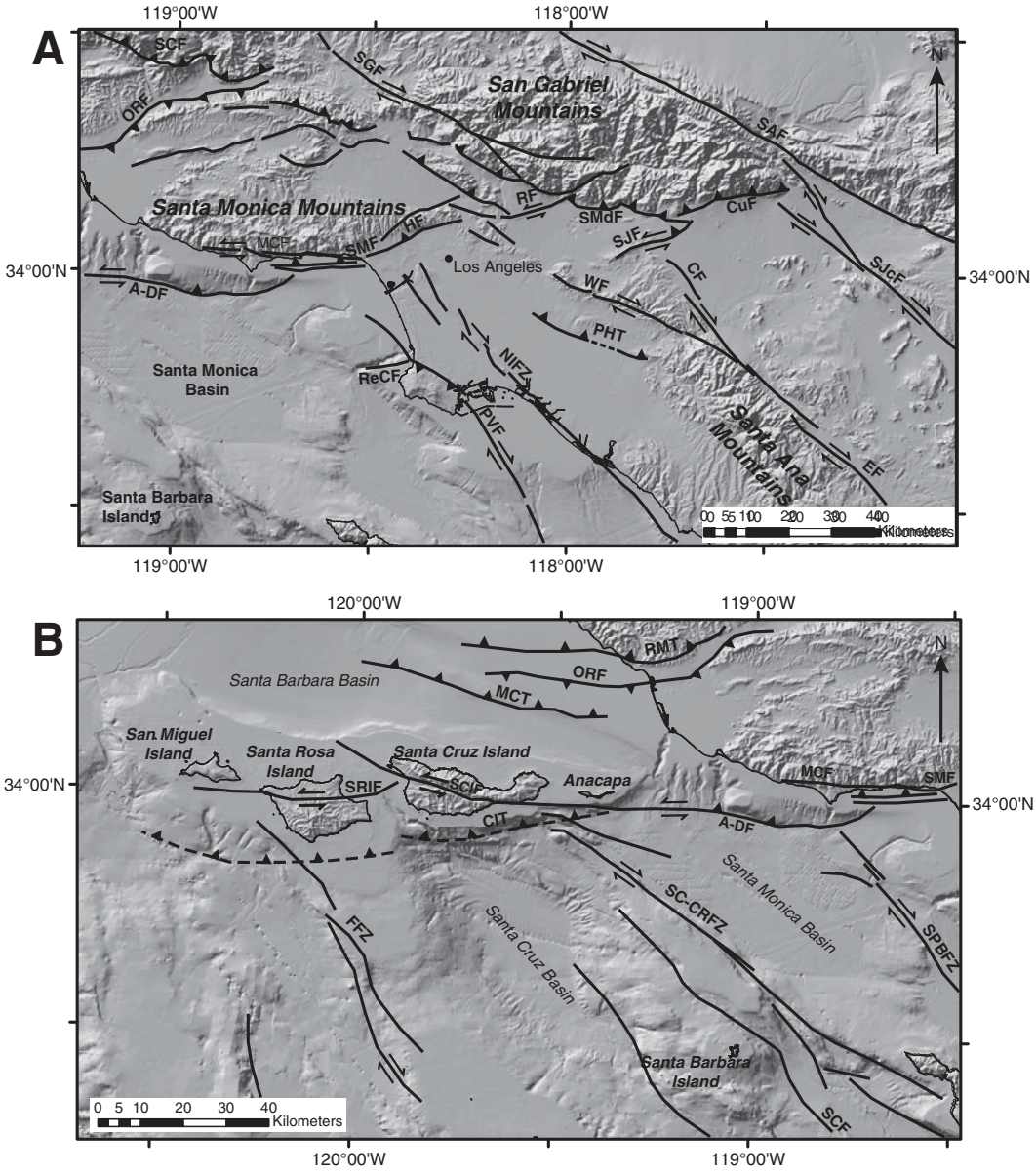

Figure 2. (A) Simplified map of the major onshore and nearshore fault systems of the Los Angles basin and vicinity, showing the style of fault interactions at the boundary between the left-oblique and south-vergent thrusts that dominate the Transverse Ranges and right-lateral and right-oblique Peninsular Ranges oriented blocks. (B) Simplified map of the major offshore right-oblique fault systems of the northern California Continental Borderland and left-oblique and south-vergent thrusts that dominate the Western Transverse Ranges in the vicinity of the two blocks. Abbreviations are as for Figure 1, plus: CIT—Channel Islands thrust; CuF—Cucamonga fault; HF—Hollywood fault; MCT—Mid-Channel thrust; PHT—Puente Hills thrust; ORF—Oak Ridge fault; ReCF—Redondo Canyon fault; RMT—Red Mountain thrust; SPBFZ—San Pedro basin fault zone. Traces of onshore and offshore faults modified from Jennings (1994).

Ridge). The southern boundary of the Western Transverse Ranges is marked by the left-oblique Santa Rosa Island and Santa Cruz Island faults (Fig. 2; Pinter and Sorlien, 1991; Colson et al., 1995), the offshore continuation of the Malibu Coast fault, and the northward-dipping Channel Islands (Shaw and Suppe, 1994) and Anacapa-Dume thrust faults (Seeber and Sorlien, 2000; Fisher et al., 2005a).

Our focus in this paper is the intersection of the northern end of the Santa Cruz–Catalina Ridge, and its bounding right-lateral faults, with the Northern Channel Islands platform and underlying Channel Islands thrust fault (Fig. 1A). The Santa Cruz–Catalina Ridge is a fault-bounded anticlinal ridge composed of blocks of Franciscan basement, igneous intrusives, and overlying Miocene volcanic and sedimentary rocks (Pilger, 1977; Junger, 1979). Legg et al. (2007) suggest that the Santa Cruz–Catalina Ridge is a structurally inverted Miocene basin, uplifted along preexisting Miocene extensional faults within the Pliocene and younger transpressional stress field. Complex zones of deformation, likely related to the intersection, flank the ridge on its western and eastern sides. The Northern Channel Islands platform, along with the Santa Barbara basin, is considered by Shaw and Suppe (1994) to be the southwestern extension of the Transverse Ranges, marking the active deformation front of this east-west–trending fold-thrust belt. The Northern Channel Islands platform is composed of Late Cretaceous to middle Miocene stratal sequences that are deformed into a broad east-west–trending anticlinorium with associated smaller folds, above the blind and active Channel Islands thrust. Although the Channel Islands thrust has yet to be definitively imaged with seismic-reflection techniques, Shaw and Suppe (1994) used fold geometry derived from seismic-reflection profiles to show this fault to have a ramp-flat geometry. They show a north-dipping ramp underlying the Northern Channel Islands and Santa Barbara basin that merges with near-horizontal fault surfaces that are at a depth of ~5 km south of the Northern Channel Islands platform and ~15 km below the shelf between Santa Barbara and Ventura. Shaw and Suppe (1994) calculate a slip rate on the fault of 1.3 mm/yr. Seeber and Sorlien (2000) propose a different geometry for this fault, suggesting that

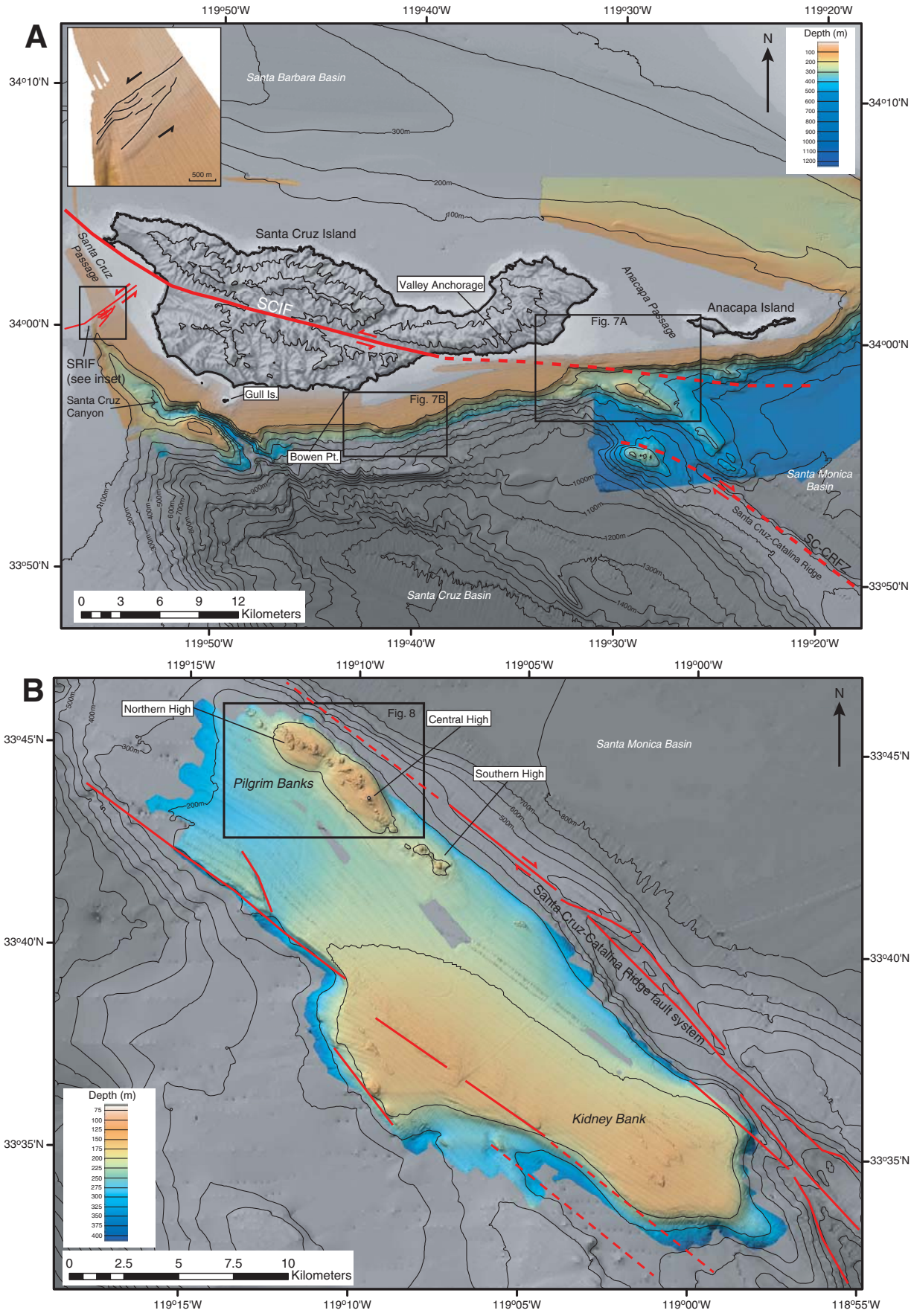
A
B
Santa Barbara Basin
Santa Cruz Island
Santa Cruz Passage
SCIF
SRIF
(see inset)
Valley Anchorage
Anacapa Passage
Anacapa Island
Fig. 7A
Fig. 7B
Gull Is.
Bowen Pt.
Santa Cruz Canyon
Santa Monica Basin
Santa Cruz-Catalina Ridge
SC-CRFZ
Santa Cruz Basin
Depth (m)
0 3 6 9 12 Kilometers
Northern High
Central High
Southern High
Fig. 8
Pilgrim Banks
Santa Cruz-Catalina Ridge fault system
Kidney Bank
0 2.5 5 7.5 10 Kilometers
119°50'W
119°40'W
119°30'W
119°20'W
34°10'N
34°00'N
33°50'N
119°15'W
119°10'W
119°05'W
119°00'W
118°55'W
33°45'N
33°40'N
33°35'N

Figure 3. (A) High-resolution multibeam bathymetry of part of the Northern Channel Islands platform, focused on the southern and western sides of Santa Cruz Island and the southern side of Anacapa Island, compiled from data collected in 2003 and 2004, with additional bathymetry around Anacapa Island from Dartnell et al. (2005) and around Gull Island from Kvitek et al. (2004). The Santa Cruz Island fault (SCIF), Santa Rosa Island fault (SRIF), and Santa Cruz–Catalina Ridge fault zone (SC-CRFZ) are shown. Contour interval is 100 m for bathymetry and 250 m for topography. Boxes show the locations of Figure 7A, B. Inset shows the stepped (en echelon) nature of the Santa Rosa Island fault as it passes north of Santa Cruz Canyon. (B) High-resolution multibeam bathymetry of the crest of the southern Santa Cruz–Catalina Ridge, with Pilgrim Banks to the north. The bathymetric high south of Pilgrim Banks is commonly referred to as Kidney Bank or Hidden Reef. Red lines show faults of the Santa Cruz–Catalina Ridge fault zone. Box shows location of Figure 8. Contour interval is 100 m.

the fault may be more listric, flattening out at a depth of ~16 km with a slip rate of 1–2 mm/yr.

DATA AND METHODS

Several recently collected data sets, including multibeam bathymetry, side-scan sonar records, and observations and samples from DELTA submersible dives are used to identify, map, and interpret submerged paleoshorelines on the Northern Channel Islands platform and Pilgrim Banks, part of the Santa Cruz–Catalina Ridge (Fig. 3).

Multibeam Bathymetry, Side-scan Imagery, and Paleoshoreline Mapping

During October 2003 and September 2004, multibeam bathymetry surveys were carried out around the Northern Channel Islands (Fig. 3A) and the Pilgrim-Kidney Banks (Fig. 3B) aboard the R/V *Velero IV*, using a pole-mounted Simrad Mesotech SM2000 imaging sonar coupled to a WAAS-enable DGPS receiver and Seatex MRU-4 attitude sensor. During these surveys this system provided data with a nominal gridded pixel resolution of 10 m for depths ranging from 30 to >400 m, with a vertical resolution of better than 3 m at depths shallower than 150 m. In post-processing, tide corrections and sound velocity profiles calculated from conductivity, temperature, and pressure (CTD) data acquired during DELTA ascents were applied to the data prior to editing. Additional multibeam bathymetric data from the National Oceanic and Atmospheric Administration (NOAA) National Geophysical Data Center (available from http://www.ngdc.noaa.gov/mgg/bathymetry/relief.html), Scripps Institution of Oceanography (available from http://nsdl.sdsc.edu), MBARI Santa Barbara basin survey (MBARI Mapping Team, 2001), California State University at Monterey Bay (Kvitek et al., 2004), and the U.S. Geological Survey (Dartnell et al., 2005) were used to fill gaps and generate grids of a wider area. In the shallow regions (<30 m) surrounding the islands where multibeam bathymetry has not yet been acquired, soundings data from NOAA National Ocean Service hydrographic surveys (available from http://www.ngdc.noaa.gov/mgg/bathymetry/relief.html) were used. Land data for the islands were derived from the 1 arc-second Shuttle Radar Topography Mission (SRTM) C-band topographic data set (Rabus et al., 2003). A final series of grids made at high resolution using the tide and sound velocity corrected data (resolution of ~15 m) and at lower resolutions using combined data available for the region (resolution of ~100 m) were produced for bathymetric analysis. Side-scan data with a 1-m pixel resolution covering most of the western end of Santa Cruz Island, the Anacapa Passage, and the shelf area north and south of Anacapa Island utilized in this study were collected by the U.S. Geological Survey using a Klein 2000 side-scan system (Cochrane et al., 2003; Cochrane et al., 2005).

Whereas the Northern Channel Islands platform shelf edge provides an approximate base datum for the LGM lowstand vertical position of the platform, a more robust marker of shoreline position at and following the LGM is required for a reliable estimate of vertical change to be made. Paleoshorelines removed from the active shoreface usually retain many of the erosional and depositional features seen on modern shorelines, commonly rocky former seacliffs and headlands with shallowly seaward-dipping benches or terraces retaining the former shore platform at their base, and, at times, remnants of beach environments. The terrace inner edge, which is the line of intersection of a cliff or outcrop with the shore platform or terrace, therefore provides a correlatable datum for previous sea level. For a well-developed shoreline to be created, relative sea level change must be close enough to zero to provide ample time for erosive forces to act on the coastal landscape. Using the compiled bathymetric data, slope breaks, knickpoints, and terraces-platforms were identified using a combination of three-dimensional (3D) bathymetric visualization, bathymetric profiles, and derived slope maps within a geographic information system (GIS). Identification of potential paleoshoreline features from bathymetry is subjective, complicated by artifacts introduced during collection and post-processing, post-formational depositional and erosional processes influencing the old shoreline, and by the inherent resolution limitations of the various data sets. Care was taken to avoid obvious artifacts during the analysis. In many cases, such as around San Miguel Island, parts of Santa Rosa Island, and the north side of Santa Cruz Island, the limited resolution of the available data prevents reliable interpretation, mapping, and comparison of continuous submerged paleoshoreline or slope-break features.

Submersible Observations and Sampling

Seventy DELTA submersible dives in support of this study were made on the Northern Channel Islands platform and Pilgrim-Kidney Bank during four cruises between 2000 and 2004 (Fig. 4). During these dives, observations were made of seafloor morphology and bottom composition to allow for the identification of paleoshorelines and structural features. As part of this dive program, 116 surficial-rock, bulk-sediment, and individual shell samples were recovered from the seafloor surrounding Santa Cruz, Santa Rosa, and the Anacapa Islands and the rocky bank top of Pilgrim Banks using the mechanical sampling arm on DELTA (claw and clam-shell scoop). Submersible navigation was acquired with an ORE Trackpoint II USBL system, with a horizontal positioning accuracy of better than 2 m relative to the ship's DGPS-derived position (average accuracy of better than 10 m). Sample collection depth was recorded in the submersible and cross-checked with dive CTD records and bathymetric data. On average, the difference between the recorded sampling depth and the measured water depth is <3 m. During sampling, focus was placed on identifying and collecting shell samples reflective of intertidal (+2 m to –0.5 m; Ricketts et al., 1985) or shallow subtidal (down to ~25–30 m) benthic environments. Targeted invertebrate intertidal fauna included the sessile mussel *(Mytilus)* and barnacle *(Balanus)* species in addition to numerous gastropod species all of which are characteristic of rocky shoreline habitats along the west coast of North

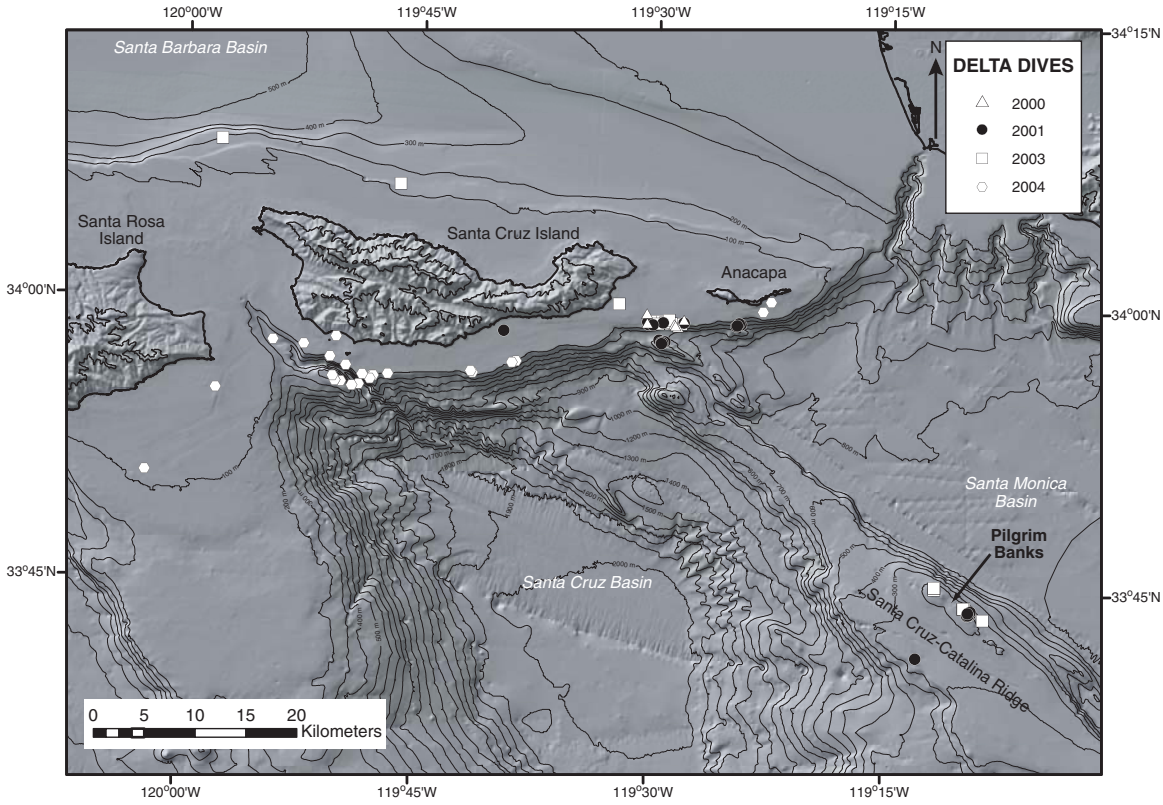

Figure 4. Locations of DELTA submersible dives made on the Northern Channel Islands platform and Santa Cruz–Catalina Ridge between 2000 and 2004. Contour interval is 100 m for bathymetry and 250 m for topography.

America. Because of the locally low numbers of these characteristic species in several areas, the shells of several species of clam that have known habitat ranges that span the intertidal and subtidal environments, such as the thick-valved clam *Humilaria kennerleyi*, were collected. Often where these few characteristic pre-modern fauna were not present, or prominent individual shell density was low, bulk sediment sampling was performed to facilitate later, more detailed analysis for species identification.

Collected samples, both individual shells and bulk skeletal sediment samples, displayed a wide range of physical conditions, from fresh looking with clear surface ornamentation and color retention, to corroded, bored, and encrusted with a complete loss of original coloring. A mix of both fresh and degraded skeletal material was found together at shallow depths, with the more degraded material dominant at greater depths. In numerous locations, articulated shells were also found. A primary consideration when using surficial shell material to date potential shoreline features is that of postmortem movement and skeletal survival of the benthic fossil assemblages characteristic of these regions (Meldahl et al., 1997). If the physical, biological, and chemical processes, including wave environment, water temperature, carbonate dissolution, and biological predation, are favorable, shell material can remain on the seafloor close to the region of initial deposition for extensive periods of time, in some cases >20 k.y. (Nelson et al., 1988). Whereas the position of collected samples cannot be unequivocally confirmed to be the site of initial postmortem deposition, the low sedimentation rates and favorable oceanographic conditions over parts of the island shelves and banks discussed here may have contributed to the preservation of surficial shell material close to the initial deposition site. Limited movement, most likely downslope, would be expected, and thus we infer that the collection depths likely represent maximum depositional depths.

AMS ^{14}C Radiocarbon Dating

Ages of shell material collected during submersible dives were obtained by accelerator mass spectrometry (AMS) ^{14}C radiocarbon dating at the Center for Accelerator Mass Spectrometry (CAMS) at Lawrence Livermore National Laboratory. The preparation and processing of these samples were carried out as described by Muzikar et al. (2003). Calib 5.0 (Stuiver and Reimer, 1993; Stuiver et al., 2005), which makes use of the IntCal04 radiocarbon calibration curve (Hughen et al., 2004), was used to correct the uncalibrated radiocarbon ages to calibrated before present (B.P.) pre-1950 ages. A reservoir correction (delta-R) of 220 ± 40 yr (Ingram and Southon, 1996) was used in this calibration for all samples except for D6169 from the Northern Channel Islands shelf (Santa Barbara basin side) for which an averaged delta-R of 268 ± 81 yr (Ingram and Southon, 1996) was used. Table 1 summarizes the identification and age information of the 42 dated samples used in this study. All ages mentioned in the following sections are the median of calibrated 2-sigma yr B.P. unless otherwise noted.

RESULTS

Eastern Northern Channel Islands Platform

The Northern Channel Islands are surrounded by a relatively flat (overall <5°), outward sloping shelf created during and after the LGM that ranges in width from ~1000 m south of Anacapa and Gull Islands (Fig. 3A) to >10,000 m north of Santa Rosa Island, except where the Santa Rosa–Cortes Ridge intersects south of Santa Rosa Island, forming a broad shelf-ridge platform. Analysis of the bathymetry shows that the

TABLE 1. AMS ^{14}C RADIOCARBON AGES OF 42 SAMPLES FROM THE NORTHERN CHANNEL ISLANDS PLATFORM AND PILGRIM BANKS

Sample ID	CAMS #	Collection Location		Sample region	Collection depth (m)	Identification	Uncorrected			Calib 5.0	
		Longitude	Latitude				^{14}C age (yr)	±	ΔR	1 sigma age yr B.P.	2 sigma age yr B.P.
D5537-1-A	103947	–119.5012	33.9808	NCI	96.0	*Puncturella cucullata*	2255	45	220±40	1530–1680	1442–1769
D5539-B1-A	104145	–119.5232	33.9801	NCI	100.0	*Nassarius* sp.	30710	230			
D5539-B2-A	104146	–119.5232	33.9801	NCI	100.0	*Nassarius* sp.	755	50	220±40	91–255	0–272
D5541-1-A	103948	–119.4914	33.9652	NCI	99.0	*Puncturella cucullata*	2065	40	220±40	1316–1450	1281–1516
D5543-1-A	104147	–119.4949	33.9635	NCI	138.0	*Ocenebra beta*	modern				
D5545-B-1	104148	–119.4903	33.9641	NCI	106.0	*Mytilus californianus*	modern				
D5545-B-2-2	117588	–119.4888	33.9630	NCI	115.0	*Nassarius insculptus*	900	30	220±40	277–386	244–450
D5546-A-1	103949	–119.1593	33.7295	PB	114.0	*Mytilus* fragments	12530	40	220±40	13709–13825	13643–13914
D5549-A-1	95866	–119.1598	33.7305	PB	121.0	*Mytilus californianus*	12280	40	220±40	13421–13586	13359–13669
D5549-B-2	95867	–119.1600	33.7300	PB	112.0	*Mytilus californianus*	11255	45	220±40	12644–12797	12570–12822
D5549-B-6	95868	–119.1600	33.7300	PB	112.0	*Mytilus californianus*	10850	35	220±40	11853–12061	11705–12117
D5550-A-2	117586	–119.1670	33.7310	PB	143.0	*Mytilus californianus*	27220	140			
D5550-A-3	117587	–119.1660	33.7310	PB	143.0	*Mytilus californianus*	26260	120			
D5550-A-4	95869	–119.1660	33.7310	PB	143.0	*Mytilus californianus*	25780	120			
D5550-hose-1	103950	–119.1660	33.7310	PB	144.0	*Megabalanus californicus*	11490	40	220±40	12829–12881	12804–12917
D6165-1	104149	–119.5096	33.9817	NCI	81.0	*Hinnites giganteus*	645	40	220±40	0–99	0–149
D6165-3/4-A	104150	–119.5169	33.9804	NCI	95.0	*Humilaria kennerleyi*	39600	600			
D6167-3-A	104151	–119.4964	33.9809	NCI	106.0	*Veneroida* sp.	26690	120			
D6169-1-B	103951	–119.4969	33.9811	NCI	99.0	*Nassarius* sp.	1390	40	220±40	661–764	629–859
D6169-1-RES	117584	–119.4969	33.9811	NCI	99.0	Partial *Conus californicus*	38000	500			
D6170-1-A	104152	–119.1936	33.7507	PB	124.0	*Humilaria kennerleyi*	16050	70	220±40	18703–18834	18632–18890
D6170-1-B	117585	–119.1936	33.7507	PB	124.0	*Nassarius* sp.	1505	35	220±40	773–894	707–931
D6170-2-A	103952	–119.1936	33.7512	PB	119.0	*Puncturella cucullata*	745	40	220±40	88–246	40–262
D6172-1	103953	–119.1939	33.7510	PB	111.0	*Megabalanus californicus*?	44400	900			
D6172-2	117583	–119.1937	33.7509	PB	119.0	*Megabalanus californicus*?	12910	35	220±40	14049–14231	13986–14523
D6173-1-A	103954	–119.1675	33.7353	PB	120.0	*Puncturella cucullata*	1350	40	220±40	636–731	560–793
D6175-1-A	103955	–119.1656	33.7341	PB	116.0	*Humilaria kennerleyi*	11925	40	220±40	13132–13235	13089–13282
D6179-3	103956	–119.7674	34.0987	NCI	90.0	*Tresus nuttallii*	14565	45	268±81	16329–16772	16140–16966
D6358-2	115206	–119.8488	33.9494	NCI	92.0	*Lucinidae* sp.	745	35	220±40	91–245	0–34/41–262
D6359-1	115207	–119.6525	33.9429	NCI	145.0	*Megabalanus californicus*	modern				
D6359-2	115208	–119.6505	33.9455	NCI	98.0	*Lucinidae* sp.?	12755	40	220±40	13895–14066	13817–14139
D6359-5	115209	–119.6456	33.9465	NCI	119.0	*Humilaria kennerleyi*	19320	60	220±40	22190–22343	22116–22420
D6359-6	115210	–119.6456	33.9465	NCI	119.0	*Humilaria kennerleyi*	18180	60	220±40	20525–20852	20445–21076
D6360-4	115211	–119.6516	33.9461	NCI	91.0	*Tresus nuttallii*	12305	40	220±40	13444–13611	13389–13692
D6361-2	115212	–119.6954	33.9341	NCI	110.0	*Lucinidae* sp.	17885	50	220±40	20268–20481	20136–20651
D6361-3	117582	–119.6958	33.9340	NCI	115.0	*Humilaria kennerleyi*	19640	60	220±40	22423–22589	22325–22694
D6361-5	115213	–119.6934	33.9350	NCI	95.0	*Humilaria kennerleyi*	20070	70	220±40	22910–23383	22699–23539
D6364-1	115214	–119.7986	33.9309	NCI	88.0	*Cerithidea* sp.	1860	35	220±40	1153–1263	1068–1292
D6365-2	115215	–119.7996	33.9282	NCI	96.0	*Puncturella cucullata*	900	35	220±40	276–390	235–460
D6373-1	115216	–119.8383	33.9249	NCI	109.0	*Humilaria kennerleyi*	14515	40	220±40	16345–16751	16172–16929
D6378-1	115217	–119.9653	33.9158	NCI	30.0	*Megabalanus californicus*	650	40	220±40	0–102	0–149
D6380-2	117581	–119.3761	33.9989	NCI	59.0	*Megabalanus californicus*	645	40			

Note: CAMS # is the Lawrence Livermore Laboratory sample identification number. ΔR is the reservoir correction. NCI—Northern Channel Islands; PB—Pilgrim Banks.

depth of the shelf edge varies across the Northern Channel Islands platform, changing from a depth of 90–100 m on the south sides of Santa Cruz Island and Anacapa Island to depths of ~90–125 m on their northern sides (Fig. 5). The shelf-edge depth increases to 120 m or deeper around San Miguel Island to the west of the study area. Below the shelf break the slopes south of Santa Cruz Island and Anacapa Island increase sharply to average values between 20° and 30° and are dissected by gullies and possible slope-failure scars in several places. It is highly likely that sections of the shelf have failed and moved downslope, with material being deposited in the Santa Monica and Santa Cruz basins, modifying or destroying sections of the oldest lowstand terraces. In comparison, the slopes below the shelf break on the northern sides of the islands are gentler and display little evidence of gully formation or slope failure, possibly a result of the higher rate of deposition and greater volume of sediment being deposited in the Santa Barbara basin.

Several prominent structures are exposed at the seafloor on the shelf, including the left-lateral oblique-slip Santa Cruz Island fault and the Santa Rosa Island fault. The surface trace of what we believe to be the Santa Cruz Island fault is seen as a distinct change in seafloor texture from rock to sediment immediately east of Valley Anchorage (Fig. 3A), where the Santa Cruz Island fault crosses the current-day Santa Cruz Island shoreline. Currently, no definitive piercing points have been identified to allow determination of slip direction or rate directly from these geophysical data. Side-scan data reveal no clearly identifiable surface rupture over this same area. The probable trace of the Santa Cruz Island fault was observed during several submersible dives (near the Valley Anchorage, Fig. 3A). In the same region, well-expressed dissected folds are visible on the bathymetric and side-scan data between Santa Cruz Island and Anacapa Island, presumably the submarine extensions of the folds mapped by Dibblee and Minch (2001a) on the eastern end of Santa Cruz and partially mapped by Junger (1979). Mapping in the Santa Cruz Passage between Santa Cruz Island and Santa Rosa Island revealed a part of the surface trace of the Santa Rosa Island fault, which displays a multi-stranded and stepped morphology just west of where it intersects the Santa Cruz Island fault (Fig. 3A inset), confirming the geometry seen by Junger (1976) from seismic-reflection profiling.

Texturally, the shelf surrounding the Northern Channel Islands is composed of a mix of

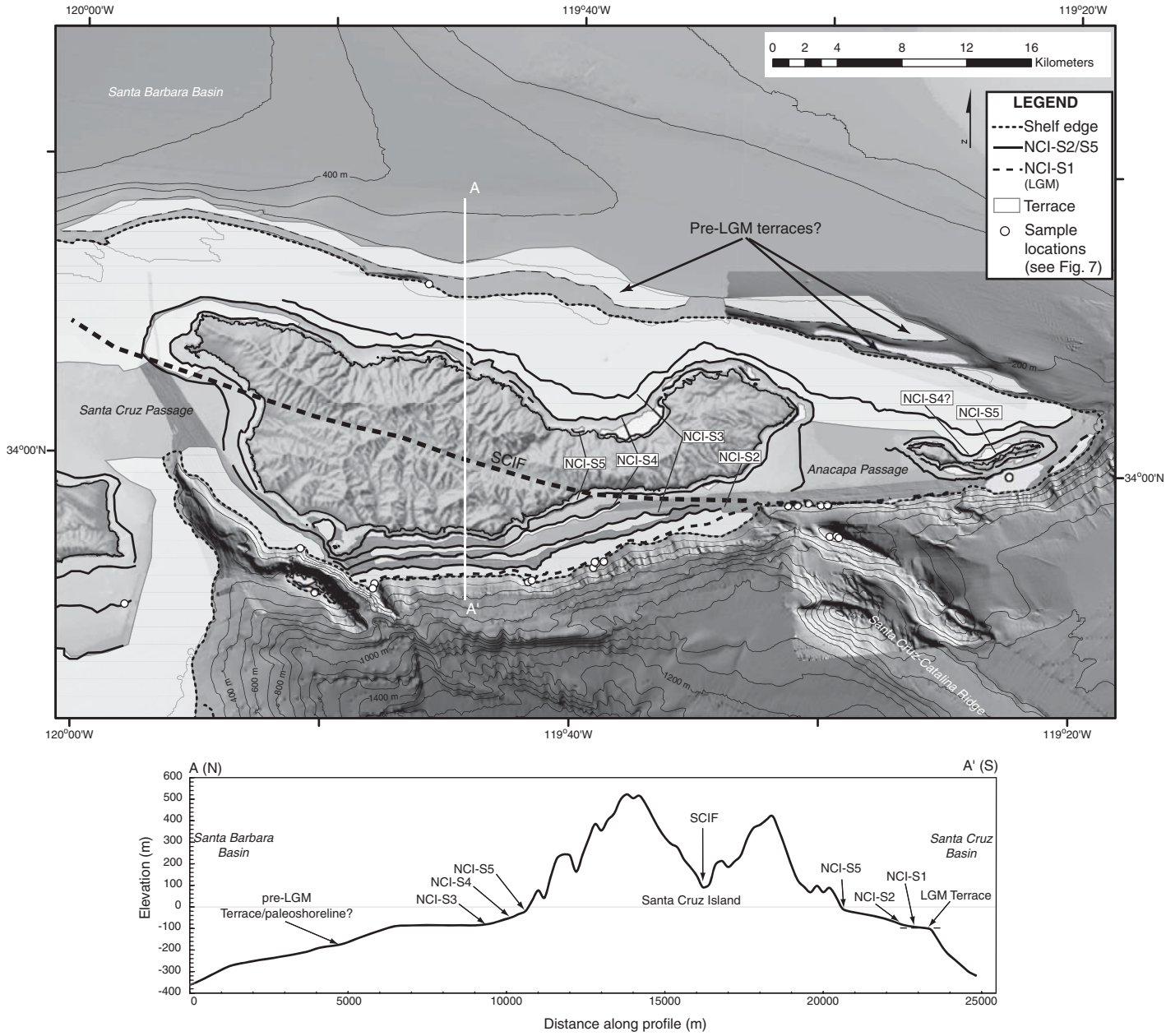

Figure 5. (A) Map of identified slope breaks and terraces of the eastern Northern Channel Islands platform, derived from analysis of bathymetric data. Potential paleoshoreline-related slope breaks are labeled NCI-S1 (LGM paleoshoreline) through NCI-S5 (paleoshoreline created just prior to the modern shoreline), with the postulated LGM paleoshoreline inner edge marked by the bolder dashed line (NCI-S1). Note that a slope break corresponding to the LGM paleoshoreline was not found on the north side of the islands, although several prominent, possibly pre-LGM benches are seen. Terrace-bench areas are white. Bathymetric contour interval is 100 m. (B) Profile A–A′ crosses the central part of Santa Cruz Island, out to the platform edges. SCIF—Santa Cruz Island fault.

fine- to coarse-grained clastic, detrital, and very fine to very coarse and larger calcareous, unconsolidated sediments deposited over and between numerous outcrops of resistant Oligocene–Miocene volcanic and sedimentary rock units (see Dibblee and Minch, 2001a, 2001b). The thicknesses of the unconsolidated sedimentary deposits vary, with the deposits on the north side of the islands commonly thicker and more laterally extensive, whereas the southern side is characteristically rockier, with areas of thin or no sediments and rare areas of thicker deposits. This is consistent with the low sediment-accumulation rates for shelf and bank-top areas of the Borderland outside the Santa Barbara basin (Gorsline and Teng, 1989; Sommerfield and Lee, 2003). The calcareous material is dominantly shell sand, composed of intact and broken shell fragments, with scattered complete and fragmental bryozoans and corals. Because the Northern Channel Islands platform is isolated by the surrounding basins from high volumes of terrigenous contributions from the major drainage systems of the mainland, there is less likelihood of these paleoshoreline deposits undergoing burial than for the shelves surrounding the mainland coast.

We recognize as many as five laterally continuous slope breaks (from the oldest, NCI-S1, to the youngest, NCI-S5) and low-angle terraces between the modern abrasion platform and the shelf-slope break surrounding parts of Santa Rosa, Santa Cruz, and Anacapa Islands, with additional assumed pre-LGM terrace levels north of Anacapa Island beyond the shelf edge (Fig. 5). Although subdued in places and masked by data artifacts, the full flight of five slope breaks is best seen on the southern, more protected side of Santa Cruz Island, where the wave environment is limited during most of the year (Gorsline and Teng, 1989) and the relatively narrow shelf provides limited space for sediment deposition. This result compares favorably with observations of Emery (1958), Scholl (1960), and Uchupi (1961), who found four to five distinct submerged terrace levels surrounding the Northern Channel Islands platform, specifically Santa Cruz Island and Anacapa Island, although the number, location, shape, and depths of the comparative shorelines and terraces differ in several places because of marked differences in data resolution. Furthermore, although the inner edges of these terraces (our paleoshorelines) commonly occur at similar depths, they are found to change depths in many locations around the islands and as such do not always follow the same bathymetric contour. As the oldest terrace surface, and because of its distinct slope break and the observed marked delineation of shelf-sediment sequence from notched or undercut rock outcroppings not seen elsewhere, we believe NCI-S1 to be the inner edge of the LGM paleoshoreline. NCI-S1 is found at a depth of ~90 m along much of the shelf south of Santa Cruz and Anacapa Islands and was the target of numerous submersible dives because of its potential for the LGM paleoshoreline.

Features characteristic of modern shoreface and nearshore environments (Bird, 2000), such as shallow-water shell and rounded pebble beaches, broken and eroded rocks and outcrops, notched and partially undercut rocky headlands, paleo-seacliffs, and horizontal wave-cut benches (Fig. 6), were found during many dives south of Santa Cruz and Anacapa Islands. In addition, accumulations of shell debris (shell hash) containing articulated shells in laterally continuous deposits, locally tens of meters in length, were observed oriented parallel and semi-parallel to mapped breaks in slope. These accumulations are morphologically similar to deposits

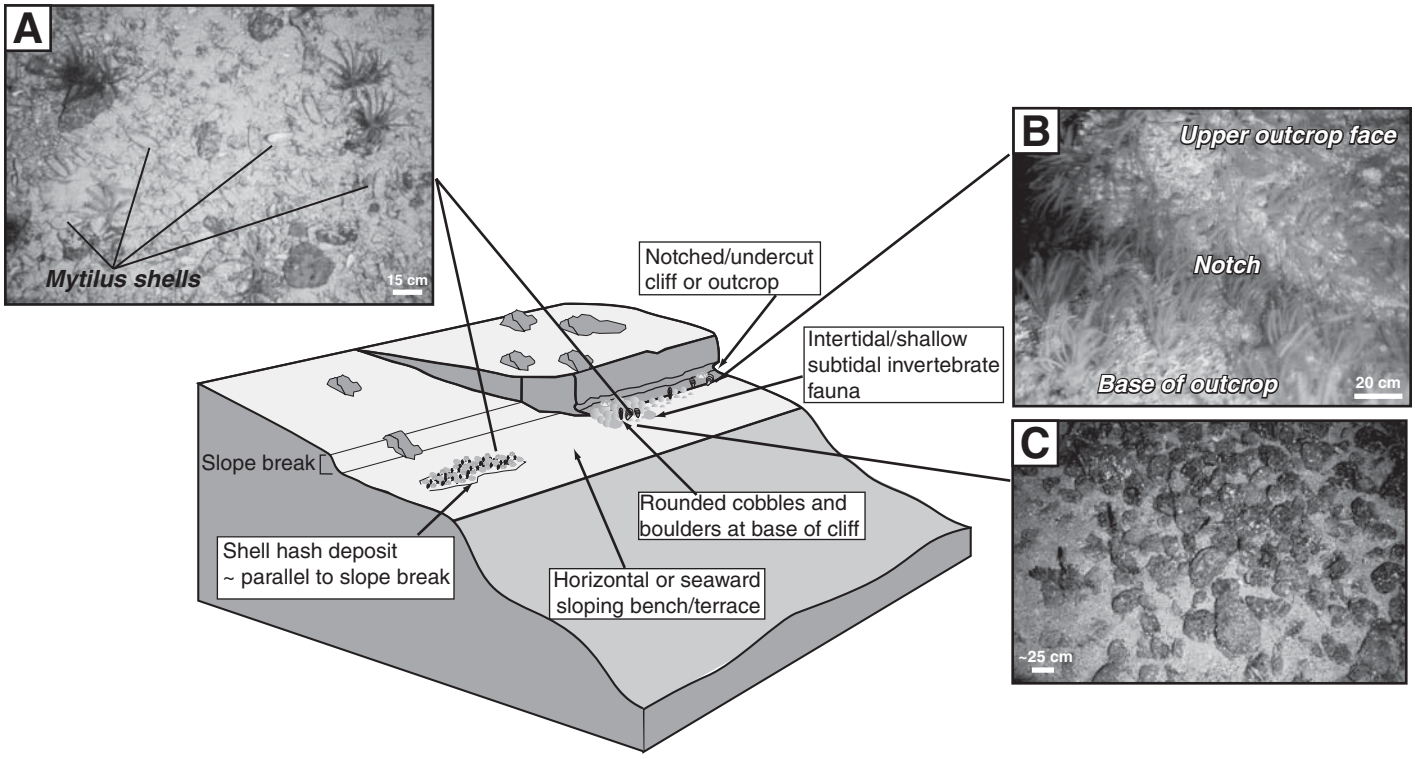

Figure 6. Composite schematic diagram of paleoshoreline features observed during submersible dives on the Northern Channel Islands platform and Pilgrim Banks. Examples of these features can be seen in photographs taken from the submersible: (A) Large, well-preserved *Mytilus californianus* shells on bench, Pilgrim Banks. (B) Notched, undercut rock outcrop on south side of Santa Cruz Island. (C) Rounded cobbles-boulders on probable paleoshoreline between Santa Cruz and Anacapa Islands, southern Northern Channel Islands platform.

generated by grain sorting within the swash and breaker zones of beaches, were submerged and partially preserved as sea level rose, and now can be used as potential paleoshoreline markers. In several locations on the south side of Santa Cruz Island and on the southern shelf edge of the Anacapa Passage between the NCI-S1 slope break and the shelf edge, a number of those features mentioned above were observed in close proximity to each other (Fig. 7A). Although evidence of these features taken individually does not always positively confirm that an area was once at sea level, especially if it has been modified subsequently by later events, the presence of several of these features together strengthens such an interpretation.

Unlike Pilgrim Banks, as discussed in the next section, no *Mytilus californianus* shells (other than a few modern examples) were found on the Northern Channel Islands platform during DELTA dives. Because these and other characteristic intertidal shells were not found, several other, less dominant intertidal and more abundant subtidal species were used to determine the age of the NCI-S1–associated 90–100-m-deep terrace and other possible paleoshorelines above this level. Of the 27 samples dated from areas of the Northern Channel Islands platform, more than half returned ages younger than 2000 yr B.P., many of which were found to be modern (<100 yr old). At the location where the Santa Cruz–Catalina Ridge and possibly the Santa Cruz Island fault intersect the Northern Channel Islands platform (Fig. 7A), samples ranging in age from modern to 39,600 ± 500 (radiocarbon yr), show various levels of shell degradation and no well-developed spatial-temporal pattern. Variable oceanographic conditions and the complex seafloor morphology within the Anacapa Passage are probably the cause of contamination of these samples by current-induced sediment transport, trapping, and mixing.

Farther east in a more protected location south of Bowen Point (Fig. 3A), several eroded, bleached, and bored samples of the subtidal clam *H. kennerleyi*, and relatively unmodified *Tresus nuttallii* (clam; habitat range down to 30 m water depth; Morris et al., 1980), and *Lucinidae* sp. were collected on the 90–100-m-deep bench and below to ~119 m. The samples in this area were found to be between 23,119 ± 420 and 13,541 ± 152 yr B.P. (Fig. 7B; Table 1). Like most other bivalve species, the habitat depth range of *H. kennerleyi* is not solidly established; they are most common in the intertidal and shallow subtidal environments, but they have been found to a depth of 45 m in places (Coan et al., 2000). No live examples of this animal were seen down to this maximum depth during the submersible dives, so we believe that those found likely grew in the intertidal to shallow-subtidal habitat range. The presence of bimodal ages at the same location, and the collection of samples below the bench with similar ages to those found on it, suggest some amount of downslope sediment movement in the area. This assumption is supported by linear textural changes visible on the side-scan imagery indicative of sediment transport. Furthermore, the younger ca. 13–14 ka ages obtained from the *T. nuttallii* (sample D6360–4) and *Lucinidae* sp. (sample D6359–2) shells from this area may be due to the more extensive habitat range of these particular fauna rather than being part of a submerged lowstand shoreline faunal assemblage. An age of 16,551 ± 379 yr B.P. was obtained from an *H. kennerleyi* shell (sample D6373–1) collected at a depth of ~110 m on the isolated ridge separated from the shelf by the Santa Cruz Channel south of Gull Island, with another post-LGM age of 16,553 ± 413 yr B.P. from a subtidal *T. nuttallii* shell (sample D6179–3) from ~90 m on the northern shelf edge of the Northern Channel Islands platform (Fig. 5).

Pilgrim Banks

Pilgrim Banks, consisting of a relatively linear, northwest-trending series of middle Miocene volcanic outcrops and pinnacles (Blanca Formation; Junger, 1979), sits atop the southern Santa Cruz–Catalina Ridge midway between the Northern Channel Islands platform and Santa Barbara Island (Figs. 1A and 3B). During the last glacial period, Pilgrim Banks may have appeared morphologically similar to Anacapa Island today, with subaerial, near-vertical, notched, and undercut cliffs, with isolated outcrops and pinnacles. The southern part of the Santa Cruz–Catalina Ridge is characterized by a broad and relatively flat top (average slope <5°) with isolated outcrops of Miocene volcanic and sedimentary strata and a relatively thin cover of Quaternary sediments. The eastern side of the ridge is bounded by strands of the active, right-oblique Santa Cruz–Catalina Ridge fault zone and on the west by northwest-striking faults and folds. The broad and flat plateau, which is at a depth of ~250 m around Pilgrim Banks, and other prominent terraces on the eastern flank of the ridge, are likely the result of pre-LGM lowstand erosion. The relatively isolated location of Pilgrim Banks from sources of terrigenous sediment, elevated well above the flanking Santa Monica and Santa Cruz depositional basins, makes it an ideal place for surface and near-surface preservation of paleoshoreline morphologic features owing to the low likelihood of contamination of inter- and subtidal organisms either from modern deposition or transported material.

Analysis of the bathymetry at Pilgrim Banks reveals two prominent slope breaks surrounding the northern and central highs (Fig. 8A) and the development of abrasion platforms at several depths. A single well-developed slope break surrounds the southern bank high of Pilgrim Banks. The shallowest slope break is found at a depth between 120 and 130 m, with the deeper one at ~140 m. The equivalent of the shelf edge surrounding the Northern Cannel Islands platform, which forms the most seaward extent of the lower terrace level, is at ~160–170 m around the northern and central bank highs. A less well defined abrasion platform, present around the pinnacle of the central high, is at ~100–105 m (Fig. 8A). During dives on the central and northern highs, notched and undercut cliff faces and well-rounded pebble-through boulder-sized rocks were observed, most notably associated with abrasion and shell-dominated depositional platforms at ~120 m.

Fifteen shell samples were dated from dives at Pilgrim Banks (Table 1; Fig. 8), predominantly the characteristic intertidal mussel *M. californianus*, whose habitat range is limited to the upper intertidal zone by *Pisaster* (sea star) predation (Paine, 1976). Although on rare occasions *M. californianus* has been found at depths below the intertidal zone where *Pisaster* abundance is low (Seed and Suchanek, 1992), no live examples were seen during submersible dives at Pilgrim Banks over the 60–250 m depth range. The lack of live *M. californianus* beyond the modern intertidal zone suggests that the fossils collected lived only in the intertidal zone before they were submerged. Additional pre-modern dates were obtained from *Megabalanus californicus* (white-ribbed barnacle, subtidal to 9 m; Morris et al., 1980) and *H. kennerleyi* shells. If the modern and near-modern ages are excluded, ages for the Pilgrim Banks samples collected between the 111 and 144 m depth range between 11,911 ± 206 and 44,000 ± 900 yr B.P. (radiocarbon [RC] ages). Three *M. californianus* samples with ages between 25,780 ± 120 (RC) and 27,220 ± 140 (RC) collected from the terrace surface at ~140 m suggest that this terrace may have been formed during the LGM lowstand.

The ages of samples recovered at depths between 110 and 120 m from outcrops along the length of the bank are found to cluster between 11,911 ± 206 and 14,255 ± 269 yr B.P. (Table 1; Figs. 8 and 9), corresponding to the sea level stillstand of the Younger Dryas. Although within the range of depth- and age-resolution

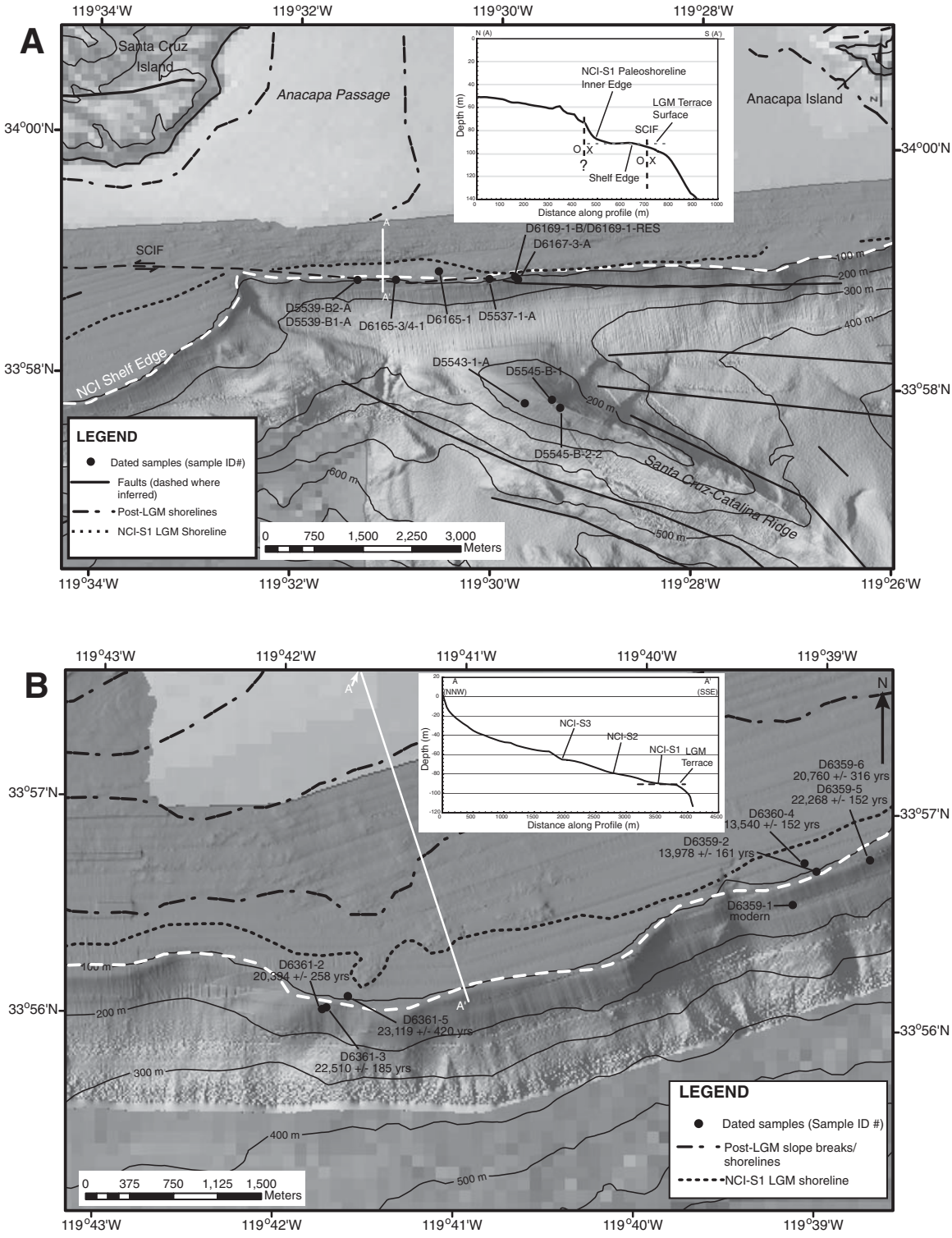

Figure 7. (A) Close-up of the bathymetry, NCI-S1 paleoshoreline, and terrace features on the southern Northern Channel Islands platform shelf edge between Santa Cruz and Anacapa Islands. The trace of the Santa Cruz Island fault (SCIF) is indicated as it crosses onto the platform, where it is likely related to destabilization of the slope. Inset: profile A–A′, showing the morphology of the cliff-back LGM terrace, with approximate locations of the Santa Cruz Island fault and an additional fault indicated (fault movement indicated by x-away, o-toward). (B) Close-up of the bathymetry, NCI-S1 paleoshoreline, and terrace features on the southern Northern Channel Islands platform shelf edge near Bowen Point, south of Santa Cruz Island. Inset: profile A–A′, showing the morphological slope breaks and terrace on this part of the platform. Bathymetric contour interval is 100 m.

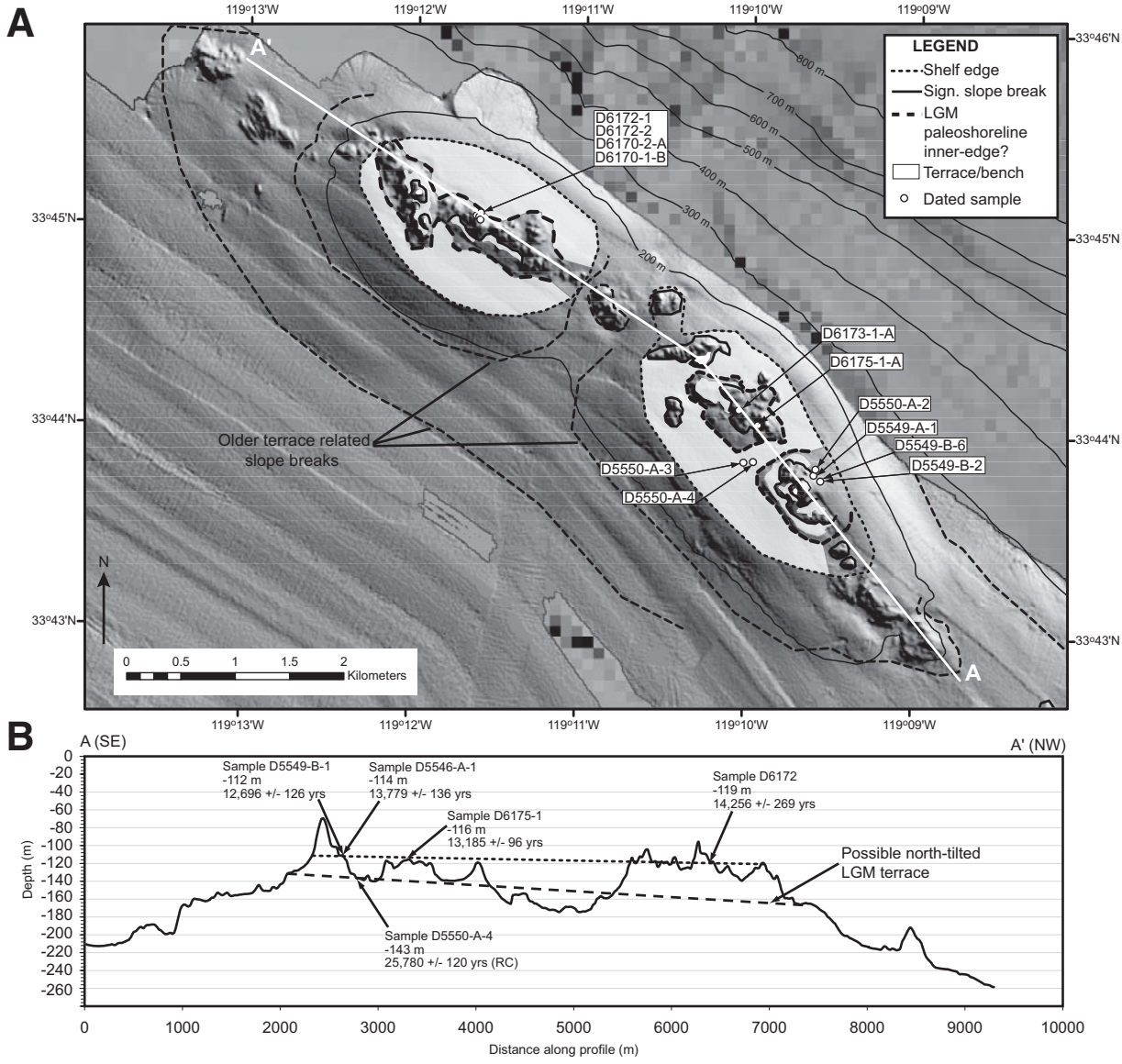

Figure 8. (A) Map of paleoshorelines and benches-terraces on Pilgrim Banks, based on analysis of the bathymetry and submersible observations. Unlike the Northern Channel Islands paleoshorelines, the slope breaks at Pilgrim Banks are not labeled because of their limited lateral continuity. Terrace-bench areas are shown in white. Possible pre-LGM inner edges–terraces are indicated. Line of profile A–A′ is indicated. Bathymetric contour interval is 100 m. (B) Southeast-northwest profile (A–A′), showing the morphology of Pilgrim Banks in relation to several of the dated shell samples. The slight increase in depth of the samples of approximately the same age (short-dashed line) and the tilt of the possible LGM terrace surface may indicate a north-directed tilt of the Santa Cruz–Catalina Ridge. RC—radiocarbon.

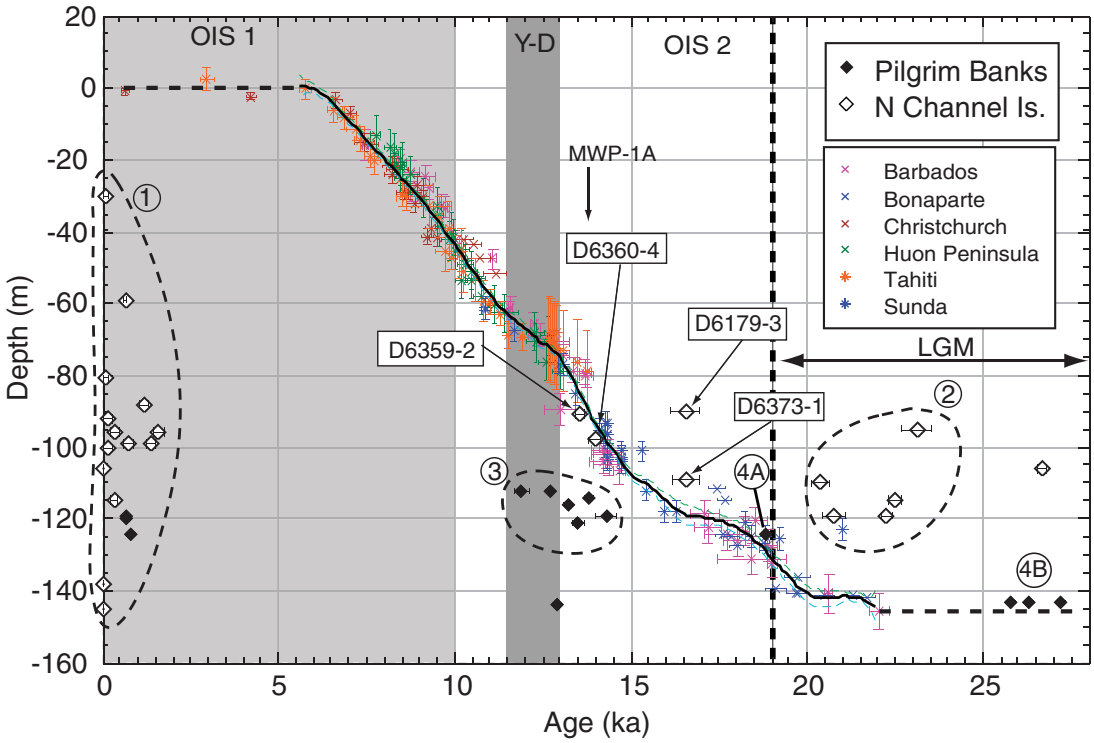

Figure 9. Linearly interpolated ice-equivalent eustatic sea-level curve for the late Pleistocene–Holocene epoch (thick black line), based on data from Lambeck et al. (2002). Upper and lower error bounds of linear fit are given (green dashed lines). Age and depth errors associated with data points as indicated by error bars. Approximate sea-level position prior to 22 ka and after 6 ka is shown by thick dashed lines. One Sunda shelf data point was removed from the linear curve fit because of its anomalous position relative to the points of the same data set. MWP-1A—melt-water pulse 1A; OIS—oxygen isotope stage; Y-D—Younger Dryas. Corrected ^{14}C radiocarbon ages of samples collected from the Northern Channel Islands platform (open diamonds) and Pilgrim Banks (filled diamonds) are shown. Two-sigma age error bars for the dated samples are shown. Note the clustering of Northern Channel Islands platform samples above the curve indicative of uplift at a rate faster than sea-level rise (group 2) and the clustering of Pilgrim Bank samples on and below the curve (group 3), indicative of submergence, or more likely, a nontectonic signal. Data points with their sample numbers indicated are discussed specifically in the text. Numbered circles: 1—dated samples not included in the analysis owing to their modern or recent ages, which may indicate depositional contamination of potential shorelines; 2—samples used in the discussion of Northern Channel Islands uplift rates; 3—samples used in the discussion of Pilgrim Banks motion; 4A and 4B—samples lying on the sea-level curve, suggesting that Pilgrim Banks has possibly not undergone vertical motion in the last 25 k.y.

error bounds, the morphology of the bank and the increasing depth at which shell material from this time period is found may reflect northward tilting of the bank (Fig. 8B) and the Santa Cruz–Catalina Ridge as a whole. The increasing depth of the lower surface, possibly formed during the LGM lowstand as indicated by the age of *M. californianus* shells discussed above, further suggests the northward tilt interpretation for the bank. It is currently not possible to determine if the tilting is the result of downward bending driven by underthrusting of the crust at the intersection, localized vertical movement along the Santa Cruz–Catalina Ridge fault system (e.g., scissoring or rotation), or some other mechanism.

DISCUSSION

Magnitude and Rate of Vertical Motion

Dated paleoshoreline features around the Northern Channel Islands platform and Pilgrim Banks provide a means of determining post-LGM vertical movements at the intersection of the Western Transverse Ranges and Borderland provinces, based on a known datum of eustatic sea level. Current estimates of eustatic sea-level rise since the end of the LGM (ca. 19 ka) vary markedly and are reported to be from 120 m (Shackleton, 2000; Peltier, 2002) to as much as 130–140 m (Yokoyama et al., 2000; Lambeck et al., 2002). Although eustatic sea level can in general be considered to represent a fixed global datum at any point in time, crustal and mantle processes related to glaciation and deglaciation can have a marked effect on coastline positions relative to sea-level height. Two of the most important of these processes are rebound from ice removal and subsidence from the increased water load following ice melting (Fleming et al., 1998; Yokoyama et al., 2000; Lambeck et al., 2002). In this analysis we use the Lambeck et al. (2002) corrected mean ice-volume equivalent eustatic sea-level data compiled from Barbados, Tahiti, the Huon Peninsula, Christchurch, Bonaparte Gulf, and the Sunda Shelf for sea level during the 22–0 ka period, which takes these processes into account. In using these sea-level

data, a similar correction to paleoshoreline positions is warranted if the net effect of post-LGM glacio-isostatic and hydrostatic readjustments in the Borderland would lead to over- or underestimation of uplift or subsidence. Although the influence of these two readjustment mechanisms on crustal motion has not been studied in detail for southern California, an estimate of glacial rebound in the region can be made. Several recent models of global and regional glacial isostatic adjustments (Peltier, 1994, 1996; Argus et al., 1999; Peltier, 2004) indicate that the crust in the southern California region may be undergoing subsidence on the order of 0.5 mm/yr, resulting from the deflation of the peripheral bulge of the Laurentian ice sheet and increasing water load. This minor subsidence value is in line with what would be expected at a site far from the ice sheet (Mitrovica and Davis, 1995; Argus et al., 1999) and, if occurring, could cause uplift rates to be underestimated or subsidence rates to be overestimated. Additionally, in a recent study of the role of sediment-load isostatic adjustment of the Northern Channel Islands platform, Pinter et al. (2003) concluded that a component of isostatic uplift driven by sediment removal may be acting on this platform, with submergence in the surrounding basins. Whereas this mechanism may be influencing the long-term uplift of the Northern Channel Islands (discussed below), we believe that its influence on the short-term signal is minor, and as such no correction of our data is made to reflect this effect.

Using the eustatic sea-level curve in Figure 9, we estimated the short-term magnitude and vertical tectonic rate of the eastern Northern Channel Islands platform and Pilgrim Banks area. Figure 9 shows the age and collection depth of samples from these two regions plotted against the simplified eustatic sea-level curve. Samples in group 1 represent modern deposition and are excluded from the following discussion. The plot of Northern Channel Islands dated samples against the eustatic sea-level curve shows a distinct grouping of the samples from and just below the 90–100 m slope break terrace (NCI-S1) between ca. 20,500 and 23,000 yr B.P. (group 2 in Fig. 9). The samples are between 20 m (D6359–6) and 45 m (D6361–5) above the expected depth (~140 m) for samples of that age. Using the average age of the group 2 samples (21,810 ± 266 yr), and assuming a constant uplift rate, the south side of the Northern Channel Islands platform would have a maximum uplift rate of 2.06 ± 0.03 mm/yr (45 m change) and a minimum of 0.92 ± 0.01 mm/yr (20 m change). Taken together, these values therefore provide an estimate of post-LGM uplift of the Santa Cruz and Anacapa Islands section of the Northern Channel Islands platform of 1.50 ± 0.59 mm/yr. This same analysis can be done with the age of the samples that correspond with the maximum and minimum differences from the expected depth. For sample D6361–5, uplift of as much as 45 m since ca. 23 ka would give an uplift rate of 1.95 ± 0.04 mm/yr. Using the minimum amount of uplift of 20 m in ca. 21,500 yr B.P. given by sample D6359–6, a minimum uplift rate of 0.96 ± 0.02 mm/yr is obtained. As before, these values taken together give an estimate of post-LGM uplift of the Santa Cruz and Anacapa Islands section of the Northern Channel Islands platform of 1.47 ± 0.52 mm/yr. Although these uplift rates closely match the 1.3 mm/yr and 1–2 mm/yr slip-rate values of the underlying Channel Islands thrust determined by Shaw and Suppe (1994) and Seeber and Sorlien (2000), respectively, we concede that its calculation is somewhat oversimplified. Except for the formal error values determined for the radiocarbon ages and the sea-level curve, these calculations do not include corrections for the possible post-glacial subsidence discussed above or for the potential error in components of the data collection and analysis such as sample collection (depth, horizontal position, timing) and bathymetric data accuracy (vertical and horizontal). Although the horizontal and vertical errors are on average less than a few meters for the sample location and bathymetric mapping systems, changes in the depth of sample collection or mapped paleoshoreline depth could result in a 5% to 15% variation in the calculated rates.

We also find our rate to be twice the uplift rate determined for the Channel Islands from uplifted marine terraces and lowstand shelf delta deposits from around the Northern Channel Islands (Pinter et al., 2003). Additionally, Pinter et al. (2003) calculated a 0.8 mm/yr isostatically driven subsidence rate for the northern flank of the Channel Islands anticlinorium based on these same lowstand delta deposits, corresponding to sections of the Santa Barbara, Santa Monica, and Santa Cruz basins, for which we have no means of comparison other than the paleoshorelines of Pilgrim Banks (see below). The apparent discordance between our uplift rate and that of Pinter et al. may be simply a reflection of differing time scales over which the rates are determined, ours being only the last 23 k.y., whereas theirs encompasses the last 400 k.y.

In this analysis we have excluded the dates obtained from the north side of the Northern Channel Islands platform and from the region south of Gull Island, which is isolated from the southern part of the Northern Channel Islands platform by the Santa Cruz Channel, because of outstanding questions about their applicability as paleoshoreline markers. The *T. nuttallii* sample (sample D6179–3 in Fig. 9) from a water depth of ~90 m from the shelf edge on the north side of Santa Cruz Island, while likely collected from what we believe to be the LGM lowstand-related terrace level, returned a date of 16,553 ± 413 yr B.P., ~2500 yr younger than the terminal phase of the LGM. The reason for this apparent discrepancy might be explained by the ability of the *T. nuttallii* clam to live well beyond the intertidal zone in water as deep as 30 m, which may have allowed it to colonize the LGM terrace well after it had already been submerged by rising sea level. The sample from south of Gull Island (sample D6373–1; 16,550 ± 379 yr B.P.) was excluded because the relationship of this isolated region to the Northern Channel Islands platform is still unclear, as it may have been structurally controlled independently. Additional data are required to determine whether these samples should be included in further analysis.

For Pilgrim Banks, two groupings are seen on the plot of sample ages against the sea-level curve (groups 3, 4a, and 4b; Fig. 9). Samples between ca. 11,500 and 14,500 yr B.P. in age, collected at depths between 110 and 120 m, all fall below the curve (group 3 in Fig. 9), which in terms of eustatic-only change indicates that they should currently be found at depths between 70 m for the youngest samples and 100 m for the oldest. Removing the eustatic signal from these results would suggest that Pilgrim Banks has submerged by as much as 40 m since the Younger Dryas, which, when taking the average age of samples in group 3 of Figure 9, gives a Holocene submergence rate of 3.03 ± 0.03 mm/yr. On the other hand, a ca. 18 ka *H. kennerleyi* sample collected at 124 m (group 4a in Fig. 9) on the northern outcrop at Pilgrim Banks and ca. 26 ka samples collected on a lower terrace level at 142 m (group 4b in Fig. 9), currently are at depths close to the predicted sea level for their ages. This mismatch in the age-depth relationship can be interpreted in two ways—either as the result of a change in the rate, polarity, and magnitude of vertical change of the ridge before and after the Younger Dryas, or as a reflection of organism growth and postmortem depositional mechanism tied to the rise in sea level.

In the first case the situation at Pilgrim Banks may reflect a nonsteady-state mechanism, such as localized changes in vertical motion of regions adjacent to strike-slip faults (e.g., scissoring). One such multiphase scenario may progress as follows. Before 18 ka, the Pilgrim Banks section of the Santa Cruz–Catalina Ridge may have been vertically stable or was possibly undergoing uplift at a rate equal to the rate of sea-level rise. At ca. 18 ka the rate of uplift may have slowed, continuing at this reduced rate

until the time of the Younger Dryas. A change in the polarity of vertical motion at or following the sea-level stillstand of the Younger Dryas may have driven a condition of bank subsidence, which resulted in samples deposited at, and subsequent to, the Younger Dryas being present at a greater depth than expected. Conversely, a simpler explanation might be that as sea level rose the intertidal fauna may have risen with it up the nearby pinnacles, with accumulation of postmortem skeletal material on terraces cut at their bases. At the time of growth of the 11.5 to 14.5 ka age samples collected at the base of pinnacles between 110 and 120 m, sea level varied between 70 and 100 m, with only the shallowest pinnacles above sea level and potentially hosting intertidal communities. It is possible that once sea level rose beyond the peaks of these outcrops, no further intertidal communities were able to colonize these outcrops, which may be the reason why no intertidal shells younger than 11.5 ka were found. The significance of this mechanism is that no complex vertical tectonic motion is required to account for the distribution of dated samples, with the LGM-age group at 140 m and the ca. 18 ka sample at 124 m reflecting sea-level position at these times, and the location of the younger age samples a result of depositional processes. This is currently our favored explanation for Pilgrim Banks, with further work required throughout the Borderland to establish the presence and extent of crustal subsidence in the region.

Deformation in the Intersection Zone

Before a full understanding of how significant the uplift of the Northern Channel Islands platform is in the accommodation of right-lateral motion along the Borderland blocks at the intersection, the role of secondary structures in the accommodation of deformation and some estimate of the amount and rate of motion that must be accommodated is required. Structures along the western and eastern sides of the Santa Cruz–Catalina Ridge show that deformation is actively occurring in the Borderland blocks, both at the intersection and to the south (Fig. 10; Junger, 1979; Crouch and Suppe, 1993; Bohannon and Geist, 1998; Fisher et al., 2005a, 2005b; Chaytor, 2006; Schindler et al., 2007). On the western side of the Santa Cruz–Catalina Ridge, northwest-trending anticlines subparallel to the ridge deform Pliocene–Quaternary and Miocene strata, which are underlain by northeast- and southwest-vergent northwest- to north-northwest–striking thrusts. East-west– and northwest-southeast–striking oblique-slip faults are found to be the dominant structures on the eastern flank of the Santa Cruz–Catalina Ridge and within the adjacent Santa Monica basin. Although piercing points are as yet not identified, seismicity shows that the northwest-southeast faults that strike parallel to the Santa Cruz–Catalina Ridge and form the principal deformation zone of the Santa Cruz–Catalina Ridge fault zone are active, right-lateral, slip-dominated structures (Corbett, 1984; Astiz and Shearer, 2000). Together, the structures at and

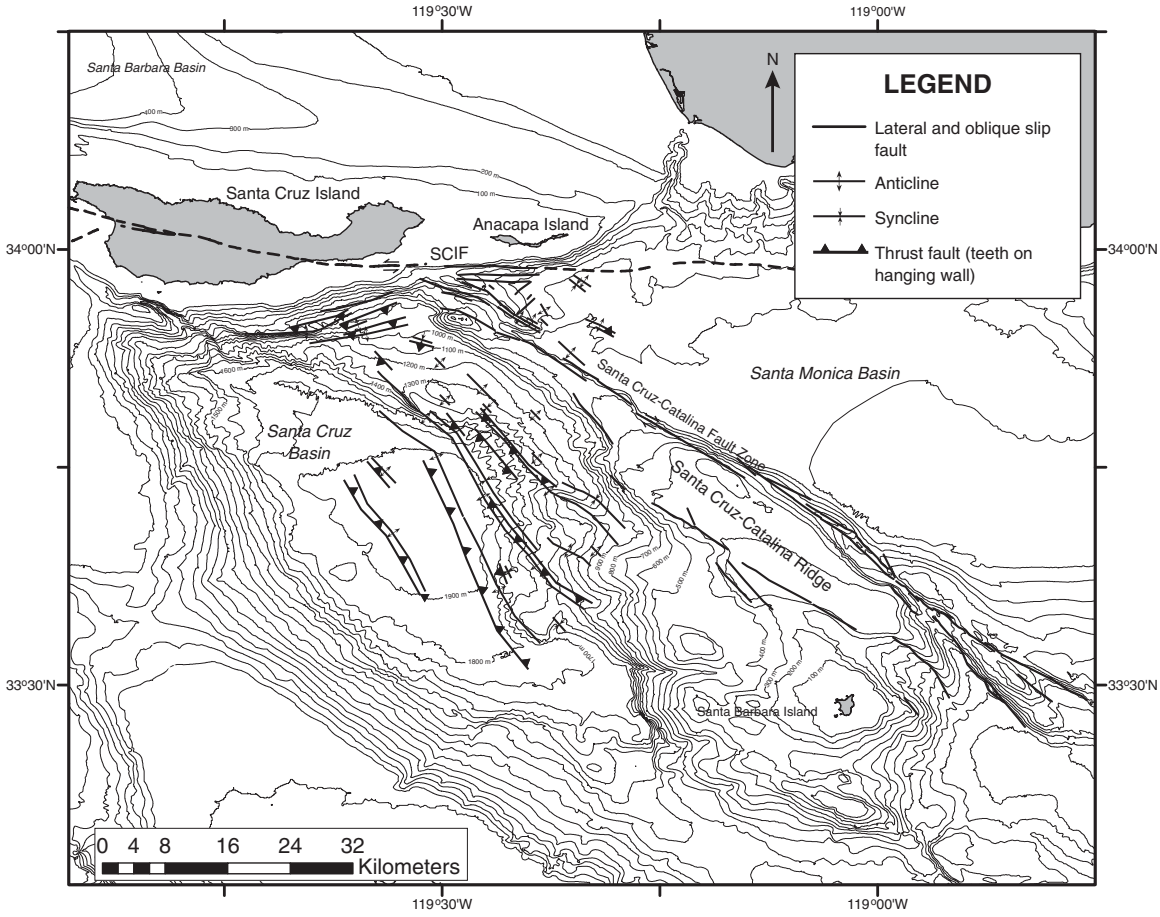

Figure 10. Preliminary map of geologic structures currently mapped using multichannel sparker, and recently released WesternGeco multichannel seismic-reflection profiles (modified from Chaytor, 2006). SCIF—Santa Cruz Island fault.

south of the intersection, especially those on the western side of the Santa Cruz–Catalina Ridge, suggest that a large component of slip on the Santa Cruz–Catalina Ridge/San Clemente fault system is being transferred onto the smaller, upper-crustal structures possibly above a crustal detachment surface.

The amount of motion needed to be accommodated either by underthrusting-uplift or deformation at and south of the intersection provides an important constraint on the significance of the uplift recorded by the NCI-S1 paleoshoreline. The structural complexity of the Borderland and the relatively limited coverage of high-resolution bathymetry and seismic-reflection data mean that few definitive piercing points are available to provide some constraints on the amount of right-lateral slip that has occurred on the northwest-southeast–trending faults of the Borderland. That said, the restoration of morphologically or sedimentologically similar features visible in the currently available data provides a mechanism for estimating the amount of slip that has occurred along these features. Using this technique, Legg (1985; 1991b) identified ~2.3 km of offset of the Boundary Fan–Slope Apron by the San Clemente fault over the last 480 yr, giving a slip rate on the order of ~4.8 mm/yr, whereas Goldfinger et al. (2000) and Legg (2005) used the offset of Emery Knoll to determine between 60 and 75 km of offset along the San Clemente fault since the middle Miocene (ca. 15 Ma; 5 mm/yr rate). This is compared with the 4 ± 3 mm/yr given by geodetic studies (Bennett et al., 1996). Although no offset features along the Santa Cruz–Catalina Ridge have yet been identified to determine a Holocene–late Pleistocene slip rate, restoration of the south end of the ridge back along the primary trace of the Santa Cruz–Catalina Ridge fault to the prominent embayment on the west side of Santa Catalina Island (Fig. 1A) provides a first-order estimate of slip on that segment of the fault of ~50 km. Although the timing of such a connection, if one existed, is unconstrained, a minimum slip rate of ~2.5 mm/yr can be estimated by assuming that separation began soon after formation of the Inner Borderland ca. 20 Ma (Bohannon and Geist, 1998). Conversely, if separation of this feature occurred once Santa Catalina Island had rotated into its current orientation, and the current transpressional regime began at ca. 5 Ma, a slip rate as high as 10 mm/yr is possible. Additionally, analysis of geodetic baselines by Shen et al. (1996) suggests that as much as 6–10 mm/yr of slip needs to be accommodated by deformation along and within the Western Transverse Ranges. Geologic (e.g., Namson and Davis, 1988) and geodetic (Larson and Webb, 1992; Larsen et al., 1993) studies show that only 6–7 mm/yr of northeast-southwest shortening is currently being accommodated by fault slip and fold growth within the frontal structural system of the Western Transverse Ranges, including the 1–2 mm/yr of slip on the Channel Islands thrust proposed by Shaw and Suppe (1994) and supported by this study.

The rate of uplift of the NCI-S1 paleoshoreline, reflecting the slip along the Channel Islands thrust, suggests that only a fraction of the motion of the Borderland blocks is being accommodated by underthrusting. The remainder must then be taken up by higher slip rates on Western Transverse Ranges faults by means of motion on other, as-yet-unidentified structural features in these ranges, continued vertical axis rotation of the ranges, or deformation at and south of the intersection of these regions. However, long-term interaction is suggested by the position of the islands on the Northern Channel Islands platform, which are consistently found west of the right-lateral fault intersections. Greater deformation and uplift of the islands, owing either to underthrusting or shallower thrusting, is expected at these locations because of the greater relative convergence rate driven by underthrusting of the active right-lateral faults. Similar deformation has been observed with subduction of active strike-slip faults (Goldfinger et al., 1997). Whether vertical fault rotation (i.e., scissoring) or flexure of the crust south of the intersection, as possibly indicated by the northward tilting of Pilgrim Banks, plays a role in accommodating any of this motion is still unclear.

CONCLUSIONS

We have used submerged LGM and younger paleoshorelines preserved around the Northern Channel Islands and Pilgrim Banks atop the Santa Cruz–Catalina Ridge to determine the vertical strain history at the intersection of two opposing structural trends in southern California. Slope breaks and terraces, which we believe to represent the LGM on the eastern Northern Channel Islands platform, indicate as much as 1.50 ± 0.59 mm/yr of late Pleistocene to Holocene uplift of the islands above the blind Channel Islands thrust. This result compares favorably with previous estimates of slip on the fault. As for Pilgrim Banks atop the Santa Cruz–Catalina Ridge, on the basis of shell ages, we currently favor an interpretation that has the ridge undergoing no vertical tectonic motion or accumulation of strain in the period since the LGM, although northward tilting of the bank may reflect flexural bending or localized structural control of the underthrust block.

Using the result from the paleoshoreline analysis, we find that although there appears to be a significant component of underthrusting at the intersection of the Western Transverse Ranges and Borderland provinces along the Channel Islands thrust interface, it may only represent a small fraction of the total amount required to accommodate northward motion of the Borderland block. It appears that a significant amount of the required contractional motion may be distributed into upper-crustal deformation and left-lateral block motion above an upper-crustal detachment, both at and south of the intersection, along the length of the major right-lateral fault systems. Much of this motion seems to be partitioned into both bending-fault termination and fold-and-thrust-belt style of deformation on the western side of the Santa Cruz–Catalina Ridge, with the development of large anticlines and listric thrust faults on the northeastern flank of the Santa Cruz basin, south of the southern margin of the Western Transverse Ranges. Although our results indicate some uplift of the Northern Channel Islands platform, they do not allow us to determine if this uplift is partitioned across the length of the platform, with the region west of the Santa Cruz–Catalina Ridge (i.e., Santa Cruz Island) uplifting at a rate different to that on the eastern side of the ridge (i.e., Anacapa Island), as could be the case on the basis of marked differences in the size of the islands.

The agreement of the rate of uplift of the eastern Northern Channel Islands platform, found through the analysis of paleoshorelines, with previous estimates of fault slip on the Channel Islands thrust, provides validation of the use of submerged paleoshorelines as an additional method of extracting the Holocene vertical tectonic component of deformation. That said, the technique currently provides results that can be greatly influenced by uncertainties inherent in underwater geophysical and sampling methods and therefore will require additional improvements and wider application to fully realize its potential.

ACKNOWLEDGMENTS

This investigation was funded under NOAA NURP awards NA03OAR4300104 and UAF030093, NOAA/UMiss award NA16RU1496-05-07-005, NOAA NMFS Southwest Fisheries Science Center SAIP award AB133F-03-SE-1279, SCEC awards USC0705036, and the 2004 SCEC summer intern program (MAM). We would like to thank Michaele Kashgarian at Lawrence Livermore National Laboratory, Paul Valentich Scott at the Santa Barbara Museum of Natural History, and Chris Chickadel, Matt Arsenault, and Alan Mix for helpful discussions. We would also like to thank the captains and crews of the R/V *Velero IV*, Delta Oceanographics, Williams & Associates, Mike Bath and Dan Francis, and the science parties for their hard work during four years of

field work. Bob Yeats, Vicki Langenheim, Brian Pratt, and an anonymous reviewer provided comments and suggestions that greatly improved this manuscript.

REFERENCES CITED

Argus, D.F., Peltier, W.R., and Watkins, M.M., 1999, Glacial isostatic adjustment observed using very long baseline interferometry and satellite laser ranging geodesy: Journal of Geophysical Research, v. 104, p. 29,077–29,093.

Astiz, L., and Shearer, P.M., 2000, Earthquake locations in the Inner Continental Borderland, offshore southern California: Bulletin of the Seismological Society of America, v. 90, p. 425–449, doi: 10.1785/0119990022.

Atwater, T., 1970, Implications of plate tectonics for the Cenozoic evolution of western North America: Geological Society of America Bulletin, v. 81, p. 3513–3536, doi: 10.1130/0016-7606(1970)81[3513:IOPTFT]2.0.CO;2.

Atwater, T., and Stock, J., 1998, Pacific–North America plate tectonics of the Neogene southwestern United States; an update: International Geology Review, v. 40, p. 375–402.

Bennett, R.A., Rodi, W., and Reilinger, R.E., 1996, Global Positioning System constraints on fault slip rates in southern California and northern Baja, Mexico: Journal of Geophysical Research, v. 101, p. 21,943–21,960, doi: 10.1029/96JB02488.

Bird, E., 2000, Coastal Geomorphology: An Introduction: New York, Wiley & Sons, 340 p.

Bohannon, R.G., and Geist, E., 1998, Upper crustal structure and Neogene tectonic development of the California Continental Borderland: Geological Society of America Bulletin, v. 110, p. 779–800, doi: 10.1130/0016-7606(1998)110<0779:UCSANT>2.3.CO;2.

Bray, N.A., Keyes, A., and Morawitz, W.M.L., 1999, The California Current system in the Southern California Bight and the Santa Barbara Channel: Journal of Geophysical Research, v. 104, p. 7695–7714, doi: 10.1029/1998JC900038.

Chaytor, J.D., 2006, Diffuse deformation patterns along the North American plate boundary zone, offshore Western United States [Ph.D. thesis]: Corvallis, Oregon State University, 299 p.

Coan, E.V., Scott, P.V., and Bernard, F.R., 2000, Bivalve Seashells of Western North America: Marine Bivalve Mollusks from Arctic Alaska to Baja California: Santa Barbara [California] Museum of Natural History, 764 p.

Cochrane, G.R., Nasby, N.M., Reid, J.A., Waltenberger, B., and Lee, K.M., 2003, Nearshore Benthic Habitat GIS for the Channel Islands National Marine Sanctuary and Southern California State Fisheries Reserves, Volume I: U.S. Geological Survey Open-File Report 03–85, http://geopubs.wr.usgs.gov/open-file/of03-85.

Cochrane, G.R., Conrad, J.E., Reid, J.A., Fangman, S., and Golden, N., 2005, The Nearshore Benthic Habitat GIS for the Channel Islands National Marine Sanctuary and Southern California State Fisheries Reserves, Volume II: U.S. Geological Survey Open-File Report 2005–1170, http://pubs.usgs.gov/of/2005/1170/.

Colson, K.B., Rockwell, T.K., Thorup, K.M., and Kennedy, G.L., 1995, Neotectonics of the left-lateral Santa Rosa Island fault, Western Transverse Ranges, southern California: Geological Society of America Abstracts with Programs, v. 27, no. 5, p. 11.

Corbett, E.J., 1984, Seismicity and crustal structure studies of southern California: Tectonic implications from improved earthquake locations [Ph.D. thesis]: Pasadena, California Institute of Technology, 231 p.

Crouch, J.K., 1979, Neogene tectonic evolution of the California Continental Borderland and western Transverse Ranges: Geological Society of America Bulletin, v. 90, p. 338–345, doi: 10.1130/0016-7606(1979)90<338:NTEOTC>2.0.CO;2.

Crouch, J.K., and Suppe, J., 1993, Late Cenozoic tectonic evolution of the Los Angeles Basin and inner California borderland; a model for core complex–like crustal extension: Geological Society of America Bulletin, v. 105, p. 1415–1434, doi: 10.1130/0016-7606(1993)105<1415:LCTEOT>2.3.CO;2.

Curray, J.R., and Moore, D.G., 1984, Tectonics and sedimentation along the California margin, *in* Crouch, J.K., and Bachman, S.B., eds., Field Trip Guidebook—Pacific Section: Society of Economic Paleontologists and Mineralogists, v. 38, p. 17–35.

Dailey, M.D., Anderson, J.W., Reish, D.J., and Gorsline, D.S., 1993, The California bight: Background and setting, *in* Dailey, M.D., et al., eds., Ecology of the Southern California Bight: A Synthesis and Interpretation: Berkeley, University of California Press, p. 1–18.

Dartnell, P., Cochrane, G.R., and Dunaway, M.E., 2005, Multibeam Bathymetry and Backscatter Data: Northeastern Channel Islands Region, Southern California: U.S. Geological Survey Open-File Report 2005–1153, http://pubs.usgs.gov/of/2005/1153/.

Dibblee, T.W., and Minch, J.A., 2001a, Geologic Map of Eastern Santa Cruz Island, Santa Barbara, California: Santa Barbara, California, Dibblee Geological Foundation Map DF-77, scale 1:24,000, 1 sheet.

Dibblee, T.W., and Minch, J.A., 2001b, Geologic Map of Western Santa Cruz Island, Santa Barbara, California: Santa Barbara, California, Dibblee Geological Foundation Map DF-77, scale 1:24,000, 1 sheet.

Dickinson, W.R., 2001, Paleoshoreline record of relative Holocene sea levels on Pacific islands: Earth-Science Reviews, v. 55, p. 191–234, doi: 10.1016/S0012-8252(01)00063-0.

Dickinson, W.R., and Snyder, W.S., 1979, Geometry of triple junctions related to San Andreas transform: Journal of Geophysical Research, v. 84, p. 561–572, doi: 10.1029/JB084iB02p00561.

Dolan, J.F., Sieh, K., and Rockwell, T.K., 2000a, Late Quaternary activity and seismic potential of the Santa Monica fault system, Los Angeles, California: Geological Society of America Bulletin, v. 112, p. 1559–1581, doi: 10.1130/0016-7606(2000)112<1559:LQAASP>2.0.CO;2.

Dolan, J.F., Stevens, D., and Rockwell, T.K., 2000b, Paleoseismologic evidence for an early to mid-Holocene age of the most recent surface rupture on the Hollywood Fault, Los Angeles, California: Bulletin of the Seismological Society of America, v. 90, p. 334–344, doi: 10.1785/0119990096.

Emery, K.O., 1958, Shallow submerged marine terraces of southern California: Geological Society of America Bulletin, v. 69, p. 39–59, doi: 10.1130/0016-7606(1958)69[39:SSMTOS]2.0.CO;2.

Engebretson, D.C., Cox, A., and Gordon, R.C., 1985, Relative Motions between Oceanic and Continental Plates: Geological Society of America Special Paper 206, 59 p.

Fisher, M.A., Normark, W.R., Bohannon, R.G., Sliter, R.W., and Calvert, A.J., 2003, Geology of the continental margin beneath Santa Monica Bay, Southern California, from seismic reflection data: Bulletin of the Seismological Society of America, v. 93, p. 1955–1983, doi: 10.1785/0120020019.

Fisher, M.A., Langenheim, V.E., Sorlien, C.C., Dartnell, P., Sliter, R.W., Cochrane, G.R., and Wong, F.L., 2005a, Recent deformation along the offshore Malibu coast, Dume, and related faults west of Point Dume, Southern California: Bulletin of the Seismological Society of America, v. 95, p. 2486–2500, doi: 10.1785/0120050042.

Fisher, M.A., Langenheim, V.E., Sorlein, C.C., Nicholson, C., and Sliter, R.W., 2005b, Active deformation along the south boundary of the Western Transverse Ranges province, Point Dume to the northern Channel Islands, southern California: Eos (Transactions, American Geophysical Union), v. 86, no. 52, abstract T51D-1362.

Fleming, K., Johnston, P., Zwartz, D., Yokoyama, Y., Lambeck, K., and Chappell, J., 1998, Refining the eustatic sea-level curve since the Last Glacial Maximum using far- and intermediate-field sites: Earth and Planetary Science Letters, v. 163, p. 327–342, doi: 10.1016/S0012-821X(98)00198-8.

Goldfinger, C., Kulm, L.D., Yeats, R.S., McNeill, L.C., and Hummon, C., 1997, Oblique strike-slip faulting of the central Cascadia submarine forearc: Journal of Geophysical Research, v. 102, p. 8217–8243, doi: 10.1029/96JB02655.

Goldfinger, C., Legg, M.R., and Torres, M.E., 2000, New mapping and submersible observations of recent activity on the San Clemente Fault: Eos (Transactions, American Geophysical Union), v. 81, no. 48, Fall Meeting Supplement, p. 1069.

Gorsline, D.S., and Teng, L.S.Y., 1989, The California Continental Borderland, *in* Winterer, E.L., et al., eds., The Eastern Pacific Ocean and Hawaii: Boulder, Colorado, Geological Society of America, Geology of North America, v. N, p. 471–487.

Hauksson, E., 1990, Earthquakes, faulting, and stress in the Los Angeles Basin: Journal of Geophysical Research, v. 95, p. 15,365–15,394, doi: 10.1029/JB095iB10p15365.

Hickey, B.M., 1992, Circulation over the Santa Monica–San Pedro Basin and Shelf: Progress in Oceanography, v. 30, p. 37–115, doi: 10.1016/0079-6611(92)90009-O.

Hughen, K.A., Baillie, M.G.L., Bard, E., Beck, J.W., Bertrand, C.J.H., Blackwell, P.G., Buck, C.E., Burr, G.S., Cutler, K.B., Damon, P.E., Edwards, R.L., Fairbanks, R.G., Friedrich, M., Guilderson, T.P., Kromer, B., McCormac, G., Manning, S., Ramsey, C.B., Reimer, P.J., Reimer, R.W., Remmele, S., Southon, J.R., Stuiver, M., Talamo, S., Taylor, F.W., van der Plicht, J., and Weyhenmeyer, C.E., 2004, Marine04 marine radiocarbon age calibration, 0–26 cal kyr BP: Radiocarbon, v. 46, p. 1059–1086.

Ingram, B.L., and Southon, J.R., 1996, Reservoir ages in Eastern Pacific coastal and estuarine waters: Radiocarbon, v. 38, p. 573–582.

Jennings, C.W., 1994, The Fault Activity Map of California and Adjacent Areas: California Geological Survey Geologic Data Map 6, scale 1:750,000, 1 sheet.

Junger, A., 1976, Offshore structure between Santa Cruz and Santa Rosa islands: American Association of Petroleum Geologists Miscellaneous Publication, Pacific Section, v. 24, p. 418–426.

Junger, A., 1979, Maps and seismic profiles showing geologic structure of the northern Channel Islands platform, California Continental Borderland: U.S. Geological Survey Miscellaneous Field Studies Map MF-991, scale 1:250,000, 5 sheets.

Kvitek, R.G., Iampietro, P.J., Bretz, C.K., Thomas, K., Zurita, S., Jones, B., and Summers-Morris, E., 2004, Hydrographic Data Acquisition in Support of MLPA and MLMA Implementation. Final Report and Appendix paper: Prepared for California Department of Fish and Game, 63 p.

Lajoie, K.R., 1986, Coastal tectonics, *in* Wallace, R.E., ed., Active Tectonics: Washington, D.C., National Academies Press, p. 95–124.

Lambeck, K., Yokoyama, Y., and Purcell, A., 2002, Into and out of the last glacial maximum; sea-level change during oxygen isotope stages 3 and 2: Quaternary Science Reviews, v. 21, p. 343–360, doi: 10.1016/S0277-3791(01)00071-3.

Larsen, S.C., Agnew, D.C., and Hager, B.H., 1993, Strain accumulation in the Santa Barbara Channel; 1970–1988: Journal of Geophysical Research, v. 98, p. 2119–2133, doi: 10.1029/92JB02043.

Larson, K.M., and Webb, F.H., 1992, Deformation in the Santa Barbara Channel from GPS measurements 1987–1991: Geophysical Research Letters, v. 19, p. 1491–1494, doi: 10.1029/92GL01485.

Legg, M.R., 1985, Geologic structure and tectonics of the inner continental borderland, offshore northern Baja California, Mexico [Ph.D. thesis]: Santa Barbara, University of California, 410 p.

Legg, M.R., 1991a, Developments in understanding the tectonic evolution of the California Continental Borderland, *in* Osborne, R.H., ed., From Shoreline to Abyss: SEPM (Society for Sedimentary Geology), Shepard Commemorative Volume, v. 46, p. 291–312.

Legg, M.R., 1991b, Sea beam evidence of Recent tectonic activity in the California Continental Borderland, *in* Dauphin, J.P., and Simoneit, B.R.T., eds., The Gulf and Peninsular Province of the Californias: American Association of Petroleum Geologists Memoir 47, p. 179–196.

Legg, M.R., 2005, Geologic slip on offshore San Clemente fault, Southern California, understated in GPS data: Eos (Transactions, American Geophysical Union), v. 86, no. 52, Fall Meeting Supplement, Abstract G53A–0876.

Legg, M.R., Kamerling, M.J., and Francis, R.D., 2004, Termination of strike-slip faults at convergence zones within continental transform boundaries: Examples from the California Continental Borderland, *in* Grocott, J., et al., eds., Vertical Coupling and Decoupling in the Lithosphere: Geological Society [London] Special Publication 227, p. 65–82.

Legg, M.R., Goldfinger, C., Kamerling, M.J., Chaytor, J.D., and Einstein, D.E., 2007, Morphology, structure and

evolution of California Continental Borderland restraining bends, *in* Cunningham, D., and Mann P., eds., Tectonics of Strike-Slip Restraining and Releasing Bends: Geological Society [London] Special Publication 290, p. 143–168.

Lynn, R.J., and Simpson, J.J., 1990, The flow of the undercurrent over the continental borderland of southern California: Journal of Geophysical Research, v. 95, p. 12,995–13,008, doi: 10.1029/JC095iC08p12995.

MBARI Mapping Team, 2001, Santa Barbara Multibeam Survey, CD-ROM: Moss Landing, California, MBARI Digital Data Series No. 4.

Meldahl, K.H., Flessa, K.W., and Cutler, A.H., 1997, Time-averaging and postmortem skeletal survival in benthic fossil assemblages; quantitative comparisons among Holocene environments: Paleobiology, v. 23, p. 209–229.

Mitrovica, J.X., and Davis, J.L., 1995, Present-day post-glacial sea level change far from the Late Pleistocene ice sheets: Implications for recent analyses of tide gauge records: Geophysical Research Letters, v. 22, p. 2529–2532, doi: 10.1029/95GL02240.

Moore, D.G., 1969, Reflection Profiling Studies of the California Continental Borderland; Structure and Quaternary Turbidite Basins: Geological Society of America Special Paper 107, 142 p.

Morris, R.H., Abbott, D.P., and Haderlie, E.C., 1980, Intertidal Invertebrates of California: Stanford, California, Stanford University Press, 690 p.

Muhs, D.R., 1983, Quaternary sea-level events on northern San Clemente Island, California: Quaternary Research, v. 20, p. 322–341, doi: 10.1016/0033-5894(83)90016-9.

Muzikar, P., Elmore, D., and Granger, D.E., 2003, Accelerator mass spectrometry in geologic research: Geological Society of America Bulletin, v. 115, p. 643–654, doi: 10.1130/0016-7606(2003)115<0643:AMSIGR>2.0.CO;2.

Namson, J., and Davis, T.L., 1988, A structural transect of the western Transverse Ranges, California: Implications for lithospheric kinematics and seismic risk evaluation: Geology, v. 16, p. 675–679, doi: 10.1130/0091-7613(1988)016<0675:STOTWT>2.3.CO;2.

Nelson, C.S., Keane, S.L., and Head, P.S., 1988, Non-tropical carbonate deposits on the modern New Zealand shelf: Sedimentary Geology, v. 60, p. 71–94, doi: 10.1016/0037-0738(88)90111-X.

Nicholson, C., Sorlien, C.C., Atwater, T., Crowell, J.C., and Luyendyk, B.P., 1994, Microplate capture, rotation of the western Transverse Ranges, and initiation of the San Andreas transform as a low-angle fault system: Geology, v. 22, p. 491–495, doi: 10.1130/0091-7613(1994)022<0491:MCROTW>2.3.CO;2.

Orr, P., 1960, Late Pleistocene marine terraces on Santa Rosa Island, California: Geological Society of America Bulletin, v. 71, p. 1113–1120, doi: 10.1130/0016-7606(1960)71[1113:LPMTOS]2.0.CO;2.

Paine, R.T., 1976, Size-limited predation: An observational and experimental approach with the *Mytilus-Pisaster* interaction: Ecology, v. 57, p. 858–873, doi: 10.2307/1941053.

Peltier, R.W., 1994, Ice age paleotopography: Science, v. 265, p. 195–201, doi: 10.1126/science.265.5169.195.

Peltier, R.W., 1996, Mantle viscosity and ice age ice sheet topography: Science, v. 273, p. 1359–1364, doi: 10.1126/science.273.5280.1359.

Peltier, R.W., 2002, On eustatic sea level history; last glacial maximum to Holocene: Quaternary Science Reviews, v. 21, p. 377–396, doi: 10.1016/S0277-3791(01)00084-1.

Peltier, R.W., 2004, Global glacial isostasy and the surface of the ice-age Earth: The ICE-5G (VM2) model and GRACE: Annual Review of Earth and Planetary Sciences, v. 32, p. 111–149, doi: 10.1146/annurev.earth.32.082503.144359.

Pilger, R.H., Jr., 1977, Structure of Santa Cruz–Catalina Ridge and adjacent areas, Southern California Continental Borderland from reflection and magnetic profiles: Implications for late Cenozoic tectonics of Southern California [Ph.D. thesis]: Los Angeles, University of Southern California, 159 p.

Pinter, N., and Sorlien, C., 1991, Evidence for latest Pleistocene to Holocene movement on the Santa Cruz Island Fault, California: Geology, v. 19, p. 909–912, doi: 10.1130/0091-7613(1991)019<0909:EFLPTH>2.3.CO;2.

Pinter, N., Lueddecke, S.B., Keller, E.A., and Simmons, K.R., 1998, Late Quaternary slip on the Santa Cruz Island Fault, California: Geological Society of America Bulletin, v. 110, p. 711–722, doi: 10.1130/0016-7606(1998)110<0711:LQSOTS>2.3.CO;2.

Pinter, N., Sorlien, C.C., and Scott, A.T., 2003, Fault-related fold growth and isostatic subsidence, California Channel Islands: American Journal of Science, v. 303, p. 300–318, doi: 10.2475/ajs.303.4.300.

Rabus, B., Eineder, M., Roth, A., and Bamler, R., 2003, The Shuttle Radar Topography Mission—A new class of digital elevation models acquired by spaceborne radar: Photogrammetry and Remote Sensing, v. 57, p. 241–262, doi: 10.1016/S0924-2716(02)00124-7.

Ricketts, E.F., Calvin, J., Hedgpeth, J.W., and Phillips, D.W., 1985, Between Pacific Tides (5th edition): Stanford, California, Stanford University Press, 652 p.

Schindler, C.S., Nicholson, C., and Sorlien, C., 2007, 3D fault geometry and basin evolution in the northern continental Borderland offshore southern California: Eos (Transactions, American Geophysical Union), v. 88, no. 52, abstract T43A-1100.

Scholl, D.W., 1960, Relationship of the insular shelf sediments to the sedimentary environments and geology of Anacapa Island, California: Journal of Sedimentary Petrology, v. 30, p. 123–139.

Seeber, L., and Sorlien, C.C., 2000, Listric thrusts in the western Transverse Ranges, California: Geological Society of America Bulletin, v. 112, p. 1067–1079, doi: 10.1130/0016-7606(2000)112<1067:LTITWT>2.3.CO;2.

Seed, R., and Suchanek, T.H., 1992, Population and community ecology of *Mytilus*, *in* Gosling, E. ed., The Mussel *Mytilus*: Ecology, Physiology, Genetics and Culture: New York, Elsevier, p. 87–169.

Shackleton, N.J., 2000, The 100,000-year ice-age cycle identified and found to lag temperature, carbon dioxide, and orbital eccentricity: Science, v. 289, p. 1897–1902, doi: 10.1126/science.289.5486.1897.

Shaw, J.H., and Suppe, J., 1994, Active faulting and growth folding in the eastern Santa Barbara Channel, California: Geological Society of America Bulletin, v. 106, p. 607–626, doi: 10.1130/0016-7606(1994)106<0607:AFAGFI>2.3.CO;2.

Shen, Z.-K., Jackson, D.D., and Ge, B.X., 1996, Crustal deformation across and beyond the Los Angeles Basin from geodetic measurements: Journal of Geophysical Research, v. 101, p. 27,957–27,980, doi: 10.1029/96JB02544.

Shepard, F.P., and Emery, K.O., 1941, Submarine Topography off the California Coast; Canyons and Tectonic Interpretation: Geological Society of America Special Paper 31, 171 p.

Sommerfield, C.K., and Lee, H.J., 2003, Magnitude and variability of Holocene sediment accumulation in Santa Monica Bay, California: Marine Environmental Research, v. 56, p. 151–176, doi: 10.1016/S0141-1136(02)00329-X.

Sorlien, C.C., Pinter, N., Seeber, L., and Kamerling, M.J., 2001, Models for slip on blind thrust faults; the Santa Monica Mountains–Channel Islands thrust and anticline, California: American Association of Petroleum Geologists Bulletin, v. 85, p. 1144.

Stephenson, W.J., Rockwell, T.K., Odum, J.K., Shedlock, K.M., and Okaya, D.A., 1995, Seismic reflection and geomorphic characterization of the onshore Palos Verdes fault zone, Los Angeles, California: Bulletin of the Seismological Society of America, v. 85, p. 943–950.

Stuiver, M., and Reimer, P.J., 1993, Extended ^{14}C database and revised CALIB radiocarbon calibration program: Radiocarbon, v. 35, p. 215–230.

Stuiver, M., Reimer, P.J., and Reimer, R.W, 2005, CALIB 5.0., http://calib.qub.ac.uk/calib.

ten Brink, U.S., Zhang, J., Brocher, T.M., Okaya, D.A., Klitgord, K.D., and Fuis, G.A., 2000, Geophysical evidence for the evolution of the California inner continental borderland as a metamorphic core complex: Journal of Geophysical Research, v. 105, p. 5835–5857, doi: 10.1029/1999JB900318.

Teng, L.S., and Gorsline, D.S., 1991, Stratigraphic framework of the California Continental Borderland basins, southern California, *in* Dauphin, J.P., and Simoneit, B.R.T., eds., The Gulf and Peninsular Province of the Californias: American Association of Petroleum Geologists Memoir 47, p. 127–143.

Tsutsumi, H., Yeats, R.S., and Huftile, G.J., 2001, Late Cenozoic tectonics of the northern Los Angeles fault system, California: Geological Society of America Bulletin, v. 113, p. 454–468, doi: 10.1130/0016-7606(2001)113<0454:LCTOTN>2.0.CO;2.

Uchupi, E., 1961, Submarine geology of the Santa Rosa–Cortes Ridge: Journal of Sedimentary Petrology, v. 31, p. 534–545.

Vedder, J.G., 1987, Regional geology and petroleum potential of the Southern California Borderland, *in* Gantz, A., ed., Geology and Resource Potential of the Continental Margin of Western North America and Adjacent Ocean Basins, Beaufort Sea to Baja California: Houston, Circum-Pacific Council for Energy and Mineral Resources, p. 403–447.

Ward, S.N., and Valensise, G., 1994, The Palos Verdes terraces, California: Bathtub rings from a buried reverse fault: Journal of Geophysical Research, v. 99, p. 4485–4494, doi: 10.1029/93JB03362.

Webster, J.M., Wallace, L., Silver, E., Applegate, B., Potts, D., Braga, J.C., Riker-Coleman, K., and Gallup, C., 2004, Drowned carbonate platforms in the Huon Gulf, Papua New Guinea: Geochemistry Geophysics Geosystems, v. 5, p. Q11008, doi: 10.1029/2004GC000726.

Wright, T.L., 1991, Structural geology and tectonic evolution of the Los Angeles Basin, California, *in* Biddle, K.T., ed., Active Margin Basins: American Association of Petroleum Geologists Memoir 52, p. 35–134.

Yeats, R.S., 1968, Southern California structure, sea-floor spreading, and history of the Pacific Basin: Geological Society of America Bulletin, v. 79, p. 1693–1702, doi: 10.1130/0016-7606(1968)79[1693:SCSSSA]2.0.CO;2.

Yeats, R.S., 1973, Newport-Inglewood fault zone, Los Angeles basin, California: American Association of Petroleum Geologists Bulletin, v. 57, p. 117–133, doi: 10.1306/83D90D54-16C7-11D7-8645000102C1865D.

Yeats, R.S., 1983, Large-scale Quaternary detachments in Ventura basin, southern California: Journal of Geophysical Research, v. 88, p. 569–583, doi: 10.1029/JB088iB01p00569.

Yeats, R.S., 2004, Tectonics of the San Gabriel Basin and surroundings, Southern California: Geological Society of America Bulletin, v. 116, p. 1158–1182, doi: 10.1130/B25346.1.

Yokoyama, Y., Lambeck, K., De Deckker, P., Johnston, P., and Fifield, L.K., 2000, Timing of the Last Glacial Maximum from observed sea-level minima: Nature, v. 406, p. 713–716, doi: 10.1038/35021035.

Manuscript Received 20 August 2007
Revised Manuscript Received 6 February 2008
Manuscript Accepted 15 February 2008

Printed in the USA